Air Force Institute of Technology

AFIT Scholar

3-2022

Modeling Gadolinium Self Powered Neutron Detectors in a Transient Reactor

Alexander L. Q. Spring

Follow this and additional works at: https://scholar.afit.edu/etd

Part of the Nuclear Engineering Commons

Modeling and Validation of Gadolinium Self
Powered Neutron Detectors in a Transient
Reactor

THESIS

Alexander L.Q. Spring, Capt, USAF

AFIT-ENP-MS-22-M-111

DEPARTMENT OF THE AIR FORCE
AIR UNIVERSITY

AIR FORCE INSTITUTE OF TECHNOLOGY

Wright-Patterson Air Force Base, Ohio

AFIT-ENP-MS-22-M-111

MODELING AND VALIDATION OF GADOLINIUM SELF POWERED

NEUTRON DETECTORS IN A TRANSIENT REACTOR

THESIS

Presented to the Faculty

Department of Nuclear Engineering

Graduate School of Engineering and Management

Air Force Institute of Technology

Air University

Air Education and Training Command

in Partial Fulfillment of the Requirements for the

Degree of Master of Science in Nuclear Engineering

Alexander L.Q. Spring, B.S.

Capt, USAF

March 2022

AFIT-ENP-MS-22-M-111

MODELING AND VALIDATION OF GADOLINIUM SELF POWERED

NEUTRON DETECTORS IN A TRANSIENT REACTOR

THESIS

Alexander L.Q. Spring, B.S.
Capt, USAF

Committee Membership:

Whitman Dailey, Ph.D.
Chair

Darren Holland, Ph.D.
Member

Juan Manfredi, Ph.D.
Member

Edward Lum, Ph.D.
Member

AFIT-ENP-MS-22-M-111

Abstract

Contributions to the electron current from the three components of a gadolinium Self Powered Neutron Detector (SPND), emitter, insulator, and sheath, are identified, characterized, and quantified to provide information on how the SPND interacts within the transient neutron and photon flux of the Transient REActor Test (TREAT) to create a measurable current. These contributions are measured by defining the SPND interactions as a dose response function used within a Monte Carlo simulation of a TREAT experiment. The data obtained from the Monte Carlo simulations are then used to compare against two analytic models, developed by Jaschik and Warren, as well as the experimental results. It was found that the methodology used produced sufficiently accurate results, that the sheath has the highest total contribution to the current, and that while the analytic models sufficiently predict the emitter contribution, they have a very limited use due to not accounting for the sheath.

Table of Contents

List of Figures

List of Tables

List of Acronyms

ENDF   Evaluated Nuclear Data File

INL   Idaho National Laboratory

LANL   Los Alamos National Laboratory

MCNP®   Monte Carlo N Particle Transport

MIMIC-N Materials and Instruments Modular Irradiation Capability for Neutron
detection

NNDC   National Nuclear Data Center

SPND   Self Powered Neutron Detector

TREAT   Transient REActor Test

MODELING AND VALIDATION OF GADOLINIUM SELF POWERED
NEUTRON DETECTORS IN A TRANSIENT REACTOR

I. Introduction

1.1 Background and Problem

The Transient REActor Test (TREAT) facility at Idaho National Laboratory
(INL) has been refurbished and resumed operations in 2017 [5]. As part of the refur-
bishment and renewed operations, modeling TREAT environments and performance
has been an ongoing effort by INL and Los Alamos National Laboratory (LANL) in
order to predict the outcomes of their nuclear reactor experiments. One of the key
areas of interest is the response of the various Self Powered Neutron Detectors (SP-
NDs) within the reactor core of TREAT. SPNDs, which are small cylindrical neutron
detectors commonly present in nuclear reactors, are used to monitor the real in-core
neutron flux. Modeling their interactions within TREAT researchers to predict per-
formance. SPNDs are neutron detectors used within the core of a nuclear reactor
environment instead of other detectors due to their simple structure, small size, no
need for power, structural stability under the environments presented within reactors,
reproducible and predictable signals, and a low burn-up [6].

To run the full TREAT model, which is a Monte Carlo N Particle Transport
(MCNP®) deck consisting of thousands of constructed solid geometries, to capture
the physics and interactions that occur within the SPNDs in MCNP® would be inef-
ficient due to the large amount of calculations because of the scatters and transitions,
especially since the electrons must be turned on to model SPNDs interactions. The

TREAT model uses a very large number of constructed solid geometries, and to turn on electron interactions would be inefficient and slow. In order to model the SPNDs within TREAT, a dose response function is used to predict how likely a neutron of a given energy will provide an electron that will be measured by the detector. This thesis details modeling and the results from the dose response functions of the gadolinium SPNDs in the TREAT MCNP® model as well as the assumptions made and limitations to this project.

1.2 Research Goals

The primary goal of this research is to identify, characterize, and quantify the contributions to the electron current from the emitter, insulator, and sheath in the gadolinium SPNDs by Monte Carlo simulation and validate against real world TREAT experiments. Limitations of the model and methodology by comparing the predicted current to TREAT experimental results and the two analytical models created by Jaschik and Warren will be determined.

1.3 Definitions

This section of the thesis is to address terms specific to the problem to introduce and define the problem specific terminology that will be used throughout this document.

1.3.1 Prompt Gammas

The term 'prompt gammas' typically refers to a gamma created during a fission event. In this document, prompt gammas instead refer to gammas that are created within the SPND via neutron absorption or interaction. E.g. an (n,γ) interaction as opposed to neutrons created through internal conversion or beta decay.

2

1.3.2 External Gammas

Gammas that are created during a fission event as well as other gammas that are created throughout a reactor are important to consider. As stated before, they are typically considered prompt gammas, in this thesis, they are referred to external gammas, i.e. gammas that are born outside of the SPND.

1.3.3 Self Shielding

Self shielding in this document refers to the how deep the reactions occur within the SPND cylinder. When neutrons interact with the gadolinium, they do not travel far due to gadolinium's high cross section, so there are more interactions and absorptions that occur at the skin of the material rather than the core.

1.3.4 Local Flux Depression

Local flux depression is due to the SPND absorbing neutrons, as such there are less neutrons in the immediate vicinity of the detector compared to other areas.

1.3.5 Emitter, Insulator, and Sheath

The emitter is the center of the SPND where the majority of the reactions will occur. The insulator is in the middle of the SPND and prevents stray electrons from reaching the sheath. The sheath acts as the collector of the electrons created from the emitter and other potential sources that reach the SPND and transfers those electron a wire for signal detection.

1.3.6 Prompt and Delayed SPNDs

There are two types of SPNDs, prompt and delayed. While these SPNDs have the same basic construction of emitter, insulator, and collector components, the prompt

and delayed SPNDs differ in the emitter material that is used to interact with the neutron flux. Delayed SPNDs use emitter elements that tend to become radioactive after neutron absorption, and use the resulting electron from a beta decay release to create a current. Prompt SPNDs create the majority of their current through neutron absorption events, where the prompt gamma rays interact with atoms and create electrons via either the photoelectric effect or Compton scattering, as such these emitter elements tend to not become radioactive after neutron absorption.

Prompt SPNDs are able to react to the flux as quickly as the electronics allow [7]. The delayed SPNDs response time, however, is determined by the half-life of the beta-decaying isotope. As these detectors are typically chosen for electron efficiency rather than sensitivity to changes in a neutron flux, their response time is on the range of seconds to minutes, and that depends on the element chosen as the emitter.

1.4 Assumptions and Limitations

1.4.1 MCNP®

MCNP® is used to predict and model interactions for TREAT and the SPNDs. It is assumed that the underlying models, material compositions, and implementations of TREAT and in general used by MCNP® and in the TREAT model are sufficient.

The model of TREAT that was provided included the material composition of the SPNDs, it is assumed that the composition and construction of the gadolinium SPNDs are adequate and that MCNP® and all the data libraries adequately predict the probability of interaction and transport of the neutron, photon, and electron particles.

1.4.2 Analytical Models

The analytical models, built by Jaschik and Warren independently, assume: [8, 9]

4

- the particle flux through the SPND is steady state,

- the particle flux through the SPND is isotropic,

- the SPND emitter is the only contributor to the current, and

- there is no material burn up.

The SPND has many methods to release electrons, however, analytical models only account for the gamma interactions within the emitter. The beta decay analytical model from Warren [10] was ignored due to desiring to model a transient pulse. The transient pulse would be over in the time frame required for the SPND to contribute to the current. The external photon fluence was also ignored in these models due to not knowing that information of the TREAT experiment, so there would be nothing to compare the result to.

The analytical model also requires the use of input data, such as cross section data from Evaluated Nuclear Data File (ENDF), gamma capture information from National Nuclear Data Center (NNDC), and neutron flux data from TREAT experiments. It is assumed that the data used to populate the analytical model is sufficiently accurate.

II. Theory

The theory chapter covers how Self Powered Neutron Detectors (SPNDs) function as well as the materials and geometry chosen to construct a SPND. This chapter also goes into detail on how the analytical models presented by Jaschik and Warren work [8, 9]. This chapter also briefly overviews Transient REActor Test (TREAT) as well as showing the neutron fluence that occurs in the reactor.

2.1   SPNDs

There are two types of SPNDs, prompt and delayed. Delayed SPNDs are more typically used in power reactors due to their increased efficiency in exchange for a signal delay ranging from seconds to minutes depending on the emitter element chosen. Delayed SPNDs have have been the focus of more research due to being commonly used within power reactors. The TREAT facility, however, uses prompt SPNDs due to their ability to reflect changes in the neutron flux with a < 1 ms time resolution [1].

Prompt SPNDs are made from either gadolinium, hafnium, platinum, ytterbium, rhodium, zirconium, cobalt, and vanadium due to their desired combination of high neutron absorption cross section and low amounts of beta decay after irradiation [9]. The element chosen for a SPND will effect the efficiency, burn up, and the type of interactions that will occur. For TREAT, the SPNDs used are made of gadolinium and hafnium; however, this thesis will only focus on the gadolinium types.

A typical SPND is illustrated in Fig 1. Surrounding the emitter element is an insulator, typically Al_2O_3, and then a collector sheath, typically made out of the material Inconel 600. These are also the materials used in the TREAT SPNDs. The emitter is the notable difference between all SPNDs, and drives the types of

6

interactions that will occur to generate current as well as the efficiency of the detector. The insulator and sheath also play a significant role in the SPND response. The insulator can trap electrons as well as create a stabilized space charge electric field that defines the minimum amount of energy required for an electron to contribute to the overall current by crossing from the emitter to the collector. The region prevents electric noise from low energy electrons created by the emitter. In TREAT, this minimum energy is about 260 keV [1].
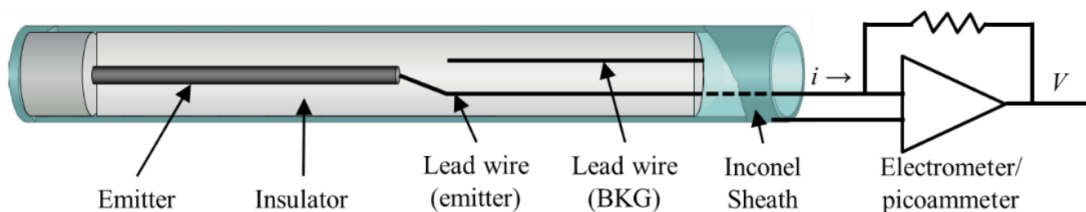
Figure 1. SPND geometry, with labeled parts [1]

This research looks at two different lengths of a gadolinium emitter in a SPNDs, these two designs will be called ILC4 and ILC6 going forward, as that is the name from TREAT. The ILC4 type SPND has the longer emitter, about four centimeters, and the ILC6 type SPND has an emitter length of about two centimeters. The specifications of the SPNDs are given in Table 1.

2.1.1 SPND Physics

SPNDs follow mostly the same process regardless if the detector is a prompt or delayed type. The process starts when a neutron enters the detector and interacts, typically with the emitter. The neutrons can be absorbed in a certain number of ways, tabulated in Table 2 [1].

Table 1. Dimensions of the Gd SPNDs

Type	Length (cm)	Inner Radius (cm)	Outer Radius (cm)
Emitter (Gd), type ILC4	4.610	N/A	0.023
Emitter (Gd), type ILC6	2.228	N/A	0.023
Insulator (Al_2O_3)	150	0.023	0.0635
Sheath (Inconel 600)	150	0.0635	0.787

Table 2. List of interactions including type and time response (ic - internal conversion, ce - Compton electron, pe - photoelectric effect

Reaction	# of Interactions	Time Response
(n, β^-)	One	Delayed
(n, e_{ic})	One	Delayed
(γ, e_{ec})	One	Prompt
(γ, e_{pe})	One	Prompt
(n, γ, e_{ec})	Two	Prompt
(n, γ, e_{pe})	Two	Prompt

Delayed SPNDs rely on the (n, β^-) reaction to generate their signal current. Prompt SPNDs generate most of their signal through the two-interaction type. Due to their reliance on gamma rays from neutrons, prompt SPNDs are also sensitive to external gamma rays [8].

Once the electrons are produced in the emitter, either from beta decay or photon interactions, they travel outward towards the collector, continuously losing energy due to inelastic collisions and the Bremsstrahlung effect. Once they get to the insulator region, they have a chance of being absorbed, especially if they do not have enough energy to overcome the space-charged electric field that is created due to the saturated insulator region. Finally they reach the collector and contribute to the detector current. This process is shown in Figure 2 [8].
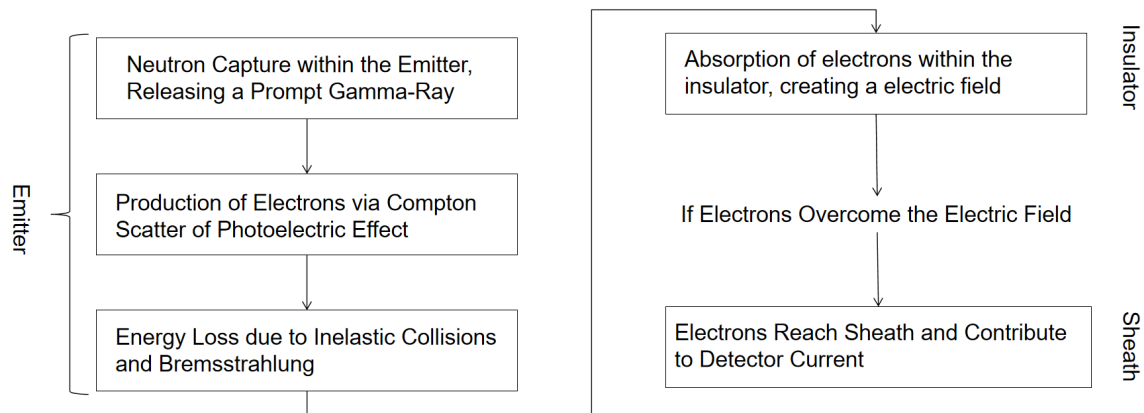
Figure 2. Process of the different interactions occurring within a prompt SPND to contribute to a detectable current.

2.1.2 Emitter, Gadolinium

The most important part of the SPND process occurs in the emitter region. The emitter material considered here is 99% pure gadolinium. In its natural state, gadolinium is composed of six stable isotopes and one radioisotope, as shown in Table 3 [11].

Table 3. Natural isotopes of gadolinium

Nuclide	Half-Life (Decay mode)	Natural Abundance
^{152}Gd	1e14 yr (α)	0.002 (1)
^{154}Gd		0.0218 (3)
^{155}Gd		0.148 (12)
^{156}Gd		0.2047 (9)
^{157}Gd		0.1565 (2)
^{158}Gd		0.2484 (7)
^{160}Gd		0.2186 (19)

Gadolinium is used in SPNDs due to its extremely high absorption of thermal neutrons. ^{157}Gd has the highest thermal neutron cross section of any stable nuclide at 259,000 barns [11]. As a comparison, hafnium, another SPND emitter used in TREAT, has a thermal neutron cross section of about 8 barns [3]. The cross sections of all the isotopes present in natural Gd are shown in Figure 3.

The major interaction for the gadolinium emitter is the probability that it will absorb the neutron. Figure 4 shows the difference between the (n,γ) cross section, and the inelastic cross section for the most significant gadolinium isotope, ^{157}Gd. As seen from Figure 4, the absorption cross section is the most important interaction as the TREAT facility is a thermal neutron reactor.

As seen in Figure 4, the other interactions are not considered important interactions. Interactions other than the neutron absorption occur at energies that are higher than what is relevant for most reactors, including the TREAT reactor. As such, neutron absorption is the interaction that should be focused on and thermalization of neutrons is important for SPND reactions to occur.
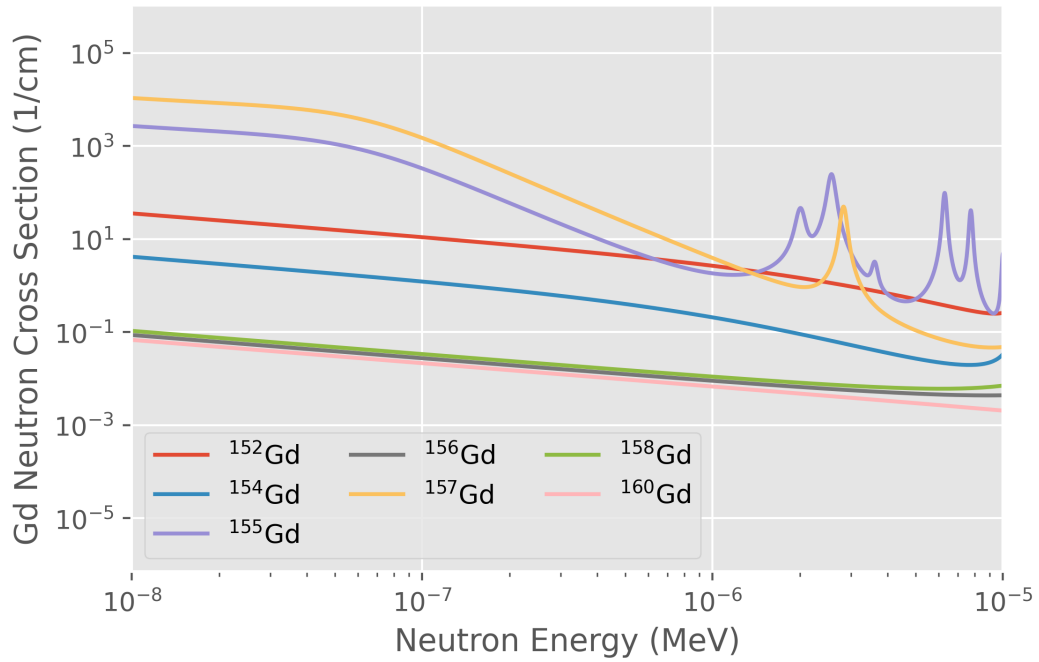
Figure 3. Absorption (n,γ) cross section of all natural occurring isotopes of gadolinium
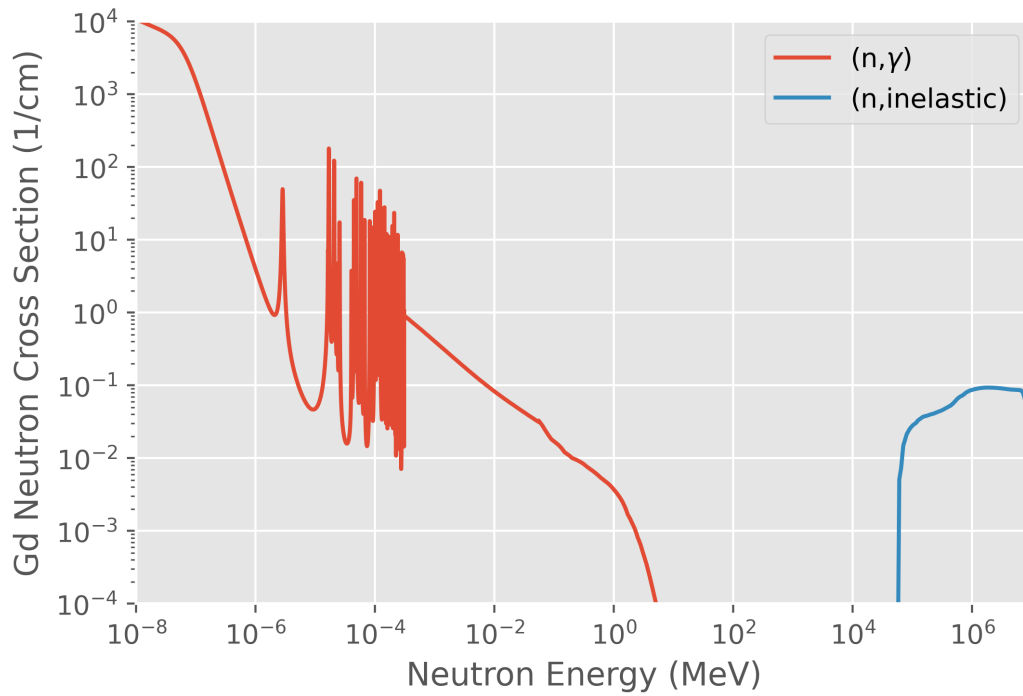
Figure 4. ^{157}Gd cross sections. Comparison between (n,γ) and inelastic scatters

It is also important to note that ^{158}Gd and ^{160}Gd have (n,β^-) reactions with emissions of 970.9 keV and 1955.8 keV beta-particles respectively. These electrons will contribute to the current once the decay time frames are relevant, where the half-lives of ^{159}Gd and ^{161}Gd are 18 hours and 3 minutes respectively [3]. These decays have been shown to have a significant effect on the current in TREAT experiments, where after about 35 minutes in a 600 kW steady state neutron flux, the gadolinium SPND's current increased by about 20% [1] due to the reaching times where beta decay reactions occur. As seen in Figure 3, the ^{158}Gd and ^{160}Gd have a cross section that is smaller than the other isotopes; however, they are guaranteed to release a high energy electron, making them much more likely to contribute to the current at a later time following absorption of a neutron.

Through the (n,γ) interaction, the gadolinium nucleus will become excited, and through de-excitation will release at least one resulting gamma particle with a maximum energy of 8.44 MeV. On average 1.67 gamma rays will be created per neutron absorption [12]. The full yield probability of a given gamma ray energy due to neutron absorption for natural gadolinium is given in Appendix A; however, a 30-group gamma energy and yield table is given in Table 4 for convenience.

After gamma rays are created through neutron absorption, they travel through the gadolinium, losing energy and creating electrons as they interact. Figure 5 shows the two major cross sections for gamma ray interactions in gadolinium: the photoelectric effect and Compton scattering. The pair production effect is not a major concern due to the low probability of occurrence as well as that the creation of a positron will, on average, create a net zero change to the current [8]. While the annihilation event will create gamma rays with high enough energies that they may contribute to the current though either the photoelectric effect or a Compton scatter, the probability of the effect occurring is too small to be considered as a notable contributor to the

current. The Compton scatters are the most dominant mode of interaction for this range of gamma ray energies, and will result in the highest contribution to the electric current due to their higher likelihood of occurrence [8].

Table 4. 30 group gamma energy and yield of natural gadolinium

Group	Average Energy (MeV)	Yield	Group	Energy Range (MeV)	Yield
1	0.0828	1.19E-1	16	0.745	1.84E-2
2	0.144	1.80E-3	17	0.791	5.02E-2
3	0.187	2.09E-1	18	0.885	9.86E-2
4	0.226	2.54E-3	19	0.954	2.05E-1
5	0.268	1.88E-2	20	1.03	7.85E-2
6	0.297	5.57E-3	21	1.15	2.65E-1
7	0.341	3.58E-3	22	1.27	1.23E-1
8	0.363	3.46E-3	23	1.45	5.84E-2
9	0.407	1.90E-3	24	1.76	7.22E-2
10	0.448	7.17E-3	25	2.06	5.87E-2
11	0.489	3.43E-3	26	2.70	1.82E-2
12	0.534	1.09E-2	27	3.85	4.24E-2
13	0.596	1.29E-2	28	4.85	3.67E-2
14	0.633	1.09E-2	29	5.36	3.88E-2
15	0.688	1.94E-2	30	6.28	7.98E-2
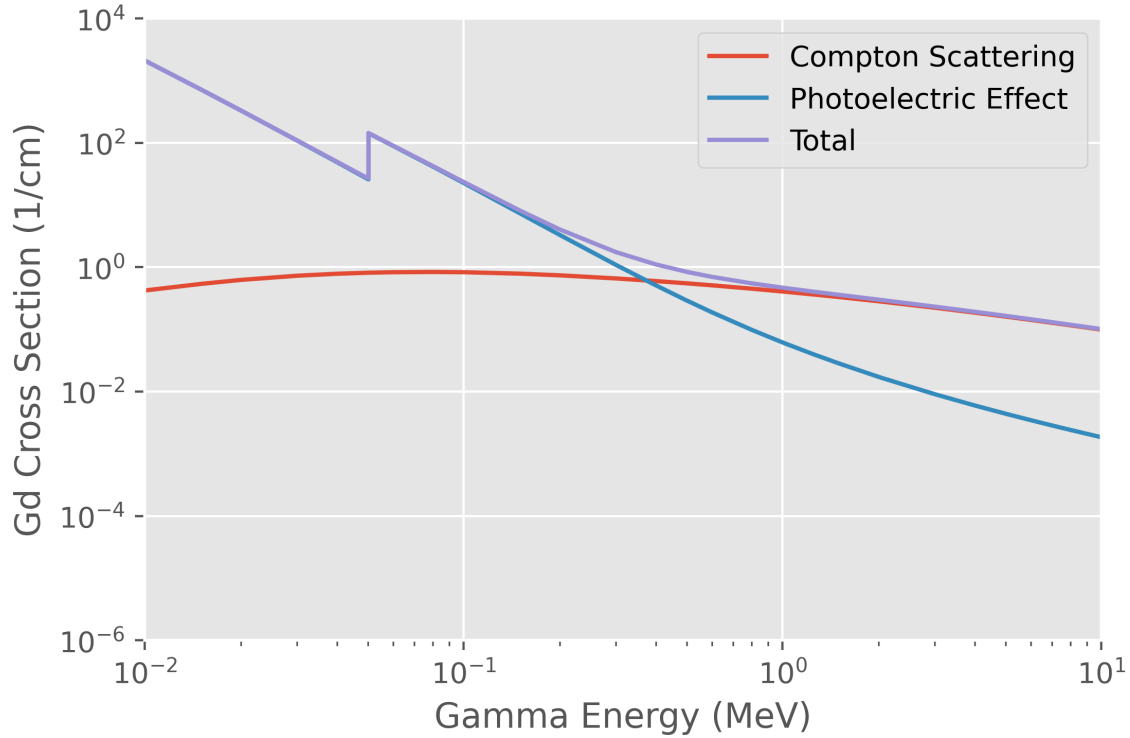
Figure 5. (γ, e^-) **Gd cross sections [2]**

2.1.3 Insulator, Aluminum Oxide and Sheath, Inconel 600

After the photon interacted with and released an electron from a gadolinium atom, the electron must travel through the insulator and into the sheath. The insulator stops thermal electrons from passing through to the collector. If the electrons get stopped in the insulator, they create an electric field. This field repels electrons away from its center, so if an electron does not have enough energy to cross it is pushed back to the emitter, and if does have enough energy it is pushed into the collector [13]. An insulator is used in SPNDs to reduce noise that would occur from allowing low energy photons created from the Bremsstrahlung effect or after many Compton scatters to contribute to the current. Once the electron passes the insulator region, it reaches the sheath, which acts as the collector. Once an electron reaches the sheath, it travels up the wire and is counted toward the SPND current. As such, especially in a prompt

14

SPND, the contributions from the insulator and sheath are important to track for as an electron created in either of those components has less space to travel (if any) to contribute to the current.

Neutrons or stray photons may interact within the insulator or sheath. As such it is important to consider the materials used in these regions as well, the TREAT gadolinium SPND insulator is made out of Aluminum Oxide with 70% density [14]. The sheath is made of Inconel 600, an alloy that is primarily made of nickel. Compared to the emitter, both of these components are relatively invisible to a thermal neutron flux due to their small cross sections, as shown in Figure 6.
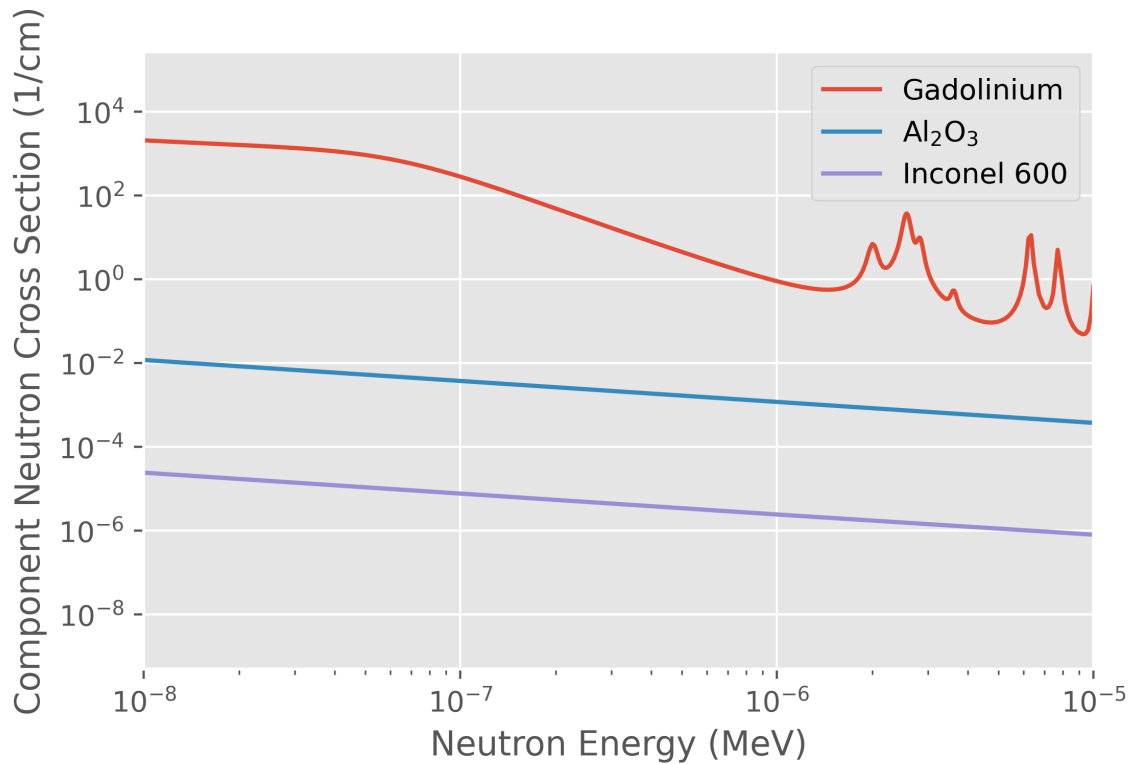
Figure 6. (n,γ) Cross sections for all SPND components [3]

As shown in Figure 6, the neutron absorption cross section for the other components is orders of magnitudes less than that of natural gadolinium. However, the neutron interaction probability is just one part of how much a component contributes

15

to the current. The gamma cross section for the other components means they may create electrons from either the gamma rays that the gadolinium do not interact with or from the external photon fluence from the reactor itself. The gamma cross sections are shown in Figure 7 and 8 for the insulator and sheath respectively.

As seen in Figures 7 and 8, these components also have a smaller gamma ray cross section than gadolinium; however, it is not as large as it was for the neutron absorption cross sections. The gamma ray cross sections for both the insulator and sheath are large enough where their volumes being much larger than the volume of the gadolinium emitter means that they will have a significant contribution to the current, especially for the sheath. Electrons created within the sheath do not have to travel in order to add to the SPND current.
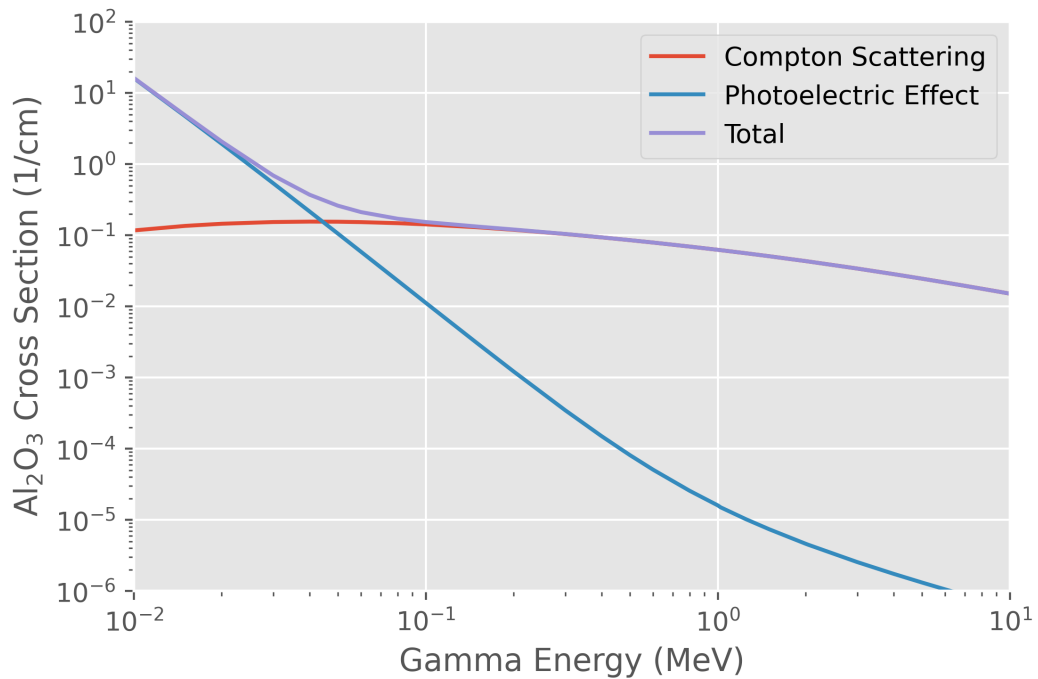
Figure 7. (γ, e^-) **Al$_2$O$_3$ cross sections** [2]
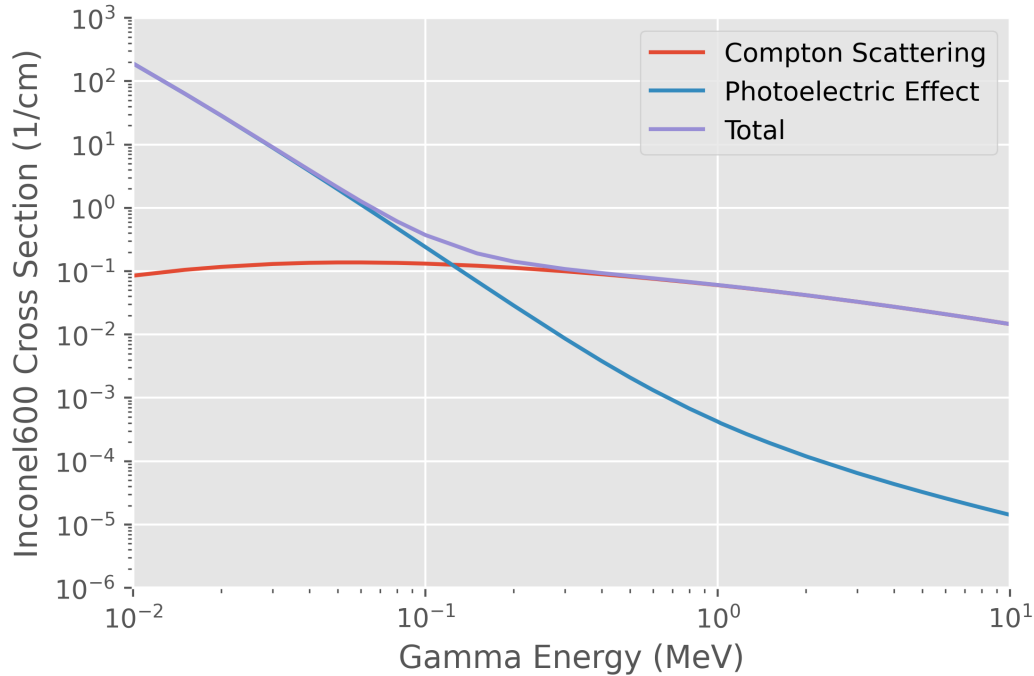
Figure 8. (γ, e^-) **Inconel 600 cross sections** [2]

2.2 Analytical Models

In order to calculate the electron current that is created from SPNDs under a high neutron flux, two analytic models were created in 1974 by Jaschik and Warren. These models only consider how many electrons are created from the emitter, as such these models may not reflect reality. The Jaschik and Warren analytic models are similar, and mostly use the same equations. There are two major differences between Jaschik and Warren [8, 9]. The first is that Warren uses approximations to reduce the computational cost required to evaluate the model. The other major difference is that Jaschik groups the prompt gamma energy and then integrates over the groups while Warren treats the prompt gammas as discrete values. It should also be noted that Warren's analytical model does address other contributions such as the (γ, e) or (n, β^-) reaction while Jaschik does not. However, only the (n, γ, e) reactions were considered due to the transient nature of the flux as well as being limited on the

17

external photon flux data within TREAT.

This section will now walk through the analytic models, with the deviations from the base equations discussed within the individual subsections.

The overall current equation for the emitter within a SPND can be given as

$$I_e = e\frac{V}{L}R_n \sum_{i=1}^{2}\left[\sum_{j=1}^{n}Y(E_{\gamma j})P_i(E_\gamma)\int_{0}^{E_{e,max}}\epsilon_i(E_e)dE_e\right] \tag{1}$$

where

I_e is the detector current in A/cm,

e is the electronic charge, 1.602E-19 A/e,

V is the volume of the emitter in cm^3,

L is the length of the emitter in cm,

R_n is the reaction rate of the flux,

$Y(E_{\gamma j})$ is the yield of a given gamma after a neutron absorption,

$P_i(E_\gamma)$ is the probability of interaction, where i indicates if it is from a Compton or photoelectric effect event, and

$\int_{0}^{E_{e,max}}\epsilon_i(E_e)dE_e$ is the electron escape efficiency over all electron energy ranges that could exist after interaction with a gamma ray of $E_{\gamma j}$.

The first term in Equation 1, R_n, denotes how likely a neutron flux is going to react with the SPND emitter. The neutron reaction rate can be described as

$$R(n) = \int_{0}^{E_{n,max}}\Sigma(E_n)\phi(E_n)f(E_n)F(E_n)dE_n \tag{2}$$

where

Σ is the macroscopic cross section of the emitter element in cm^{-1},

ϕ is the neutron flux in $n/cm^2 s$,

$f(E_n)$ is the self shielding effect, and

$F(E_n)$ is the flux depression effect.

The neutron self shielding factor, $f(E_n)$, which occurs due to the high cross section of gadolinium, impacts the reaction rate as not all of the gadolinium will be subjected to the entirety of the neutron flux. This phenomena is described in Equation 3.

$$f(E_n) = \frac{2}{3}x\Big[2\{x[K_1(x)I_1(x) + K_0(x)I_0(x)] - 1\} \\ + \frac{1}{x}K_1(x)I_1(x) - K_0(x)I_1(x) + K_1(x)I_0(x)\Big] \tag{3}$$

where $x = \Sigma(E_n)r_e$, r_e is the radius of the emitter, and I and K are modified Bessel functions of the first and second kinds, respectively.

The neutron flux depression term, $F(E_n)$, described by Equation 4 and 5, is due to neutrons interacting with the SPND. Neutrons close to the SPND are not interacting with the fissile material, so fewer neutrons are created in the immediate vicinity resulting in a lower flux local to the SPND.

$$F(E_n) = \frac{1}{1 + K_c(E_n)} \tag{4}$$

$$K_c(E_n) = \frac{3r_e}{2\lambda_{tr}}\Big[ln\big(\frac{2L}{\pi r_e}\big) - \gamma + \frac{3}{2}\Big]xf(E_n) \tag{5}$$

where λ_{tr} is the transport mean free path of the moderator used in cm, L is the average diffusion length of the moderator in cm, and γ is Euler's constant, 0.5772.

How Jashik and Warren handle the other two major terms of Equation 1 differently, the probability of interaction ($P_i(E_\gamma)$) and the escape efficiently ($\int_0^{E_{e,max}} \epsilon_i(E_e)dE_e$). They both agree on the underlying physics, however, Warren makes approximations to those two terms to lighten the calculational power required. These different formulations are addressed in the following sections.

2.2.1 Jaschik

The expression for the probability of collision is determined by representing the probability that an electron is produced by either a Compton scatter ($i = 1$) or photoelectric effect ($i = 2$). It takes into account the path length probability function, as the longer the gamma ray travels through the emitter, the more likely it is to have an electron freeing event. The expression is

$$P_i(E_\gamma) = \frac{\Sigma_i(E_\gamma)}{\Sigma_{tot}(E_\gamma)} \left\{ 1 - \int_0^{L_{max}} N(l)exp(-\Sigma_{tot}(E_\gamma)l)dl \right\} \tag{6}$$

where Σ is the macroscopic gamma ray cross section in $1/cm$, $N(l)$ is the path length probability function, and L_{max} is the maximum path length a gamma ray can have through the emitter: $\sqrt{2r_e^2 + L^2}$.

The path length probability function for a cylinder is derived in Snidow [15]. It is repeated here for clarity. It is also important to note that the exact formulation in Snidow has a samll typo, and Equation 7 is believed to be the correct formulation as it recreates the figures within Snidow's paper.

$$
\begin{aligned}
N(l) = {} & \frac{2}{\pi r_e} \int_{arcos(m)}^{arcsin(n)} sin^2(\theta)\left(1 - k^2 sin^2(\theta)\right)^{1/2} d\theta \\
& - \frac{3k}{\pi r_e \alpha} \int_{arcos(m)}^{arcsin(n)} sin^2(\theta)cos(\theta)\left(1 - k^2 sin^2(\theta)\right)^{1/2} d\theta \\
& + \frac{1}{2r_e \alpha} \int_{arcos(m)}^{arcsin(n)} sin(\theta)cos(\theta)d\theta \\
& - \frac{1}{\pi r_e \alpha} \int_{arcos(m)}^{arcsin(n)} cos(\theta)sin\big(\theta\big)arcsin(ksin(\theta))d\theta
\end{aligned} \tag{7}
$$

where

$\alpha = \frac{1}{2}L_{max}/r_e$, which is a normalized maximum path length,

$k = \frac{1}{2}l/r_e$, which is the normalized path length,

n, is the last possible angle for a normalized path length, give as 1/k or 1, de-

20

pending on if k is greater than or less than 1, respectively, and

m, is the first possible angle for a normalized path length, given as L_{max}/L or 1, depending on if k is greater than or less than 1, respectively.

The m constant in Equation 7 can be approximated as always 1 since L_{max} is very close to L for a small r_e, which is true for the geometry of the SPND emitters.

The electron escape efficiency is the probability that an electron produced within the emitter of energy E_γ will escape from the emitter, cross the insulator, and reach the collector. This efficiency is

$$\int_0^{E_{e,max}} \epsilon_i(E_e)dE_e =$$
$$\int_{E_{min}}^{E'_{max}} \left(-\frac{dE}{dx}\right) \left\{ \int_{E_{min}}^{E'_{max}} N\big[R(E') - R(E)\big]p_i(E'; E_\gamma)dE' \right\}dE \quad (8)$$

where

$\left(-\frac{dE}{dx}\right)$ is the reciprocal of the specific energy loss of electrons,

$N\big[R(E') - R(E)\big]$ is the path length probability function, where the argument is the difference in path lengths of the electron starting and ending energy,

$p_i(E'; E_\gamma)$ is the probability that a gamma ray of energy E_γ will create an electron on energy E',

E'_{max} is the maximum possible energy that a gamma ray of energy E_γ can give to an electron, and

E_{min} is the minimum energy required for an electron to travel through the insulator.

The $p_i(E'; E_\gamma)$ equation does differ significantly depending on whether it is a Compton scatter of a photoelectric effect event. The formulation for these are given

21

in Equation 9 and Equation 11 respectively.

The formulation to determine the probability of interaction for Compton scatters is

$$p_1(E'; E_\gamma) = F\left[2 + \frac{E'^2}{\beta'^2(E_\gamma - E')^2} + \frac{E'^2}{(E_\gamma - E')E_\gamma} - \frac{2E'}{\beta'(E_\gamma - E')}\right] \tag{9}$$

where F is a normalization factor, given as

$$
\begin{aligned}
F &= \frac{1}{A + B + C + D} \\
A &= E_t\left(1 + \frac{1}{\beta'}\right)^2 \\
B &= \frac{E_\gamma E_t}{\beta'^2(E_\gamma - E_t)} \\
C &= \left(\frac{2}{\beta'^2} - 1 + \frac{2}{\beta'}\right)ln\left(\frac{E_\gamma - E_t}{E_\gamma}\right)E_\gamma \\
D &= -\frac{E_t^2}{2E_\gamma}
\end{aligned}
\tag{10}
$$

where $E_t = E_\gamma \frac{2\beta'}{1+2\beta'}$ which is the maximum energy which a Compton scattered electron can gain, and $\beta' = \frac{E_\gamma}{m_0 c^2}$.

The formulation to determine the probability of interaction for the photoelectric effect is

$$p_2(E' : E_\gamma) = \delta\left[E' - (E_\gamma - E_K)\right] \tag{11}$$

where E_K is the binding energy of the on an electron in the K-shell.

As mentioned before, Jaschik groups the E_γ based on the yield function. This is done to reduce the computational cost. Jaschik groups the gamma energies through the following formulation

$$\bar{E}_\gamma = \frac{\sum_{j=1}^n E_{\gamma j} Y(E_{\gamma j})}{\sum_{j=1}^n Y(E_{\gamma j})} \tag{12}$$

Due to Jaschik grouping and integrating over the gamma ray energy yields, Equation 1 is transformed into

$$I_e = e\frac{V}{L}R_n\sum_{i=1}^{2}\left[\int_0^{E_{\gamma,max}} Y(E_\gamma)P_i(E_\gamma)\left(\int_0^{E_{e,max}}\epsilon_i(E_e)dE_e\right)dE_\gamma\right] \qquad (13)$$

2.2.2 Warren

As mentioned previously, one of the major differences between Jaschik and Warren is that Warren utilizes a lot of simplifications. This section will restate the final equations that Warren presents. And an in depth explanation for the rationale is found in Warren's article [9].The equation for the Compton scatter contribution to the component is given as

$$I_{n,\gamma,e_{ce}} = \frac{\pi}{4}edN_0\frac{KZ}{A}\bar{l}R_n\sum_{i=1}^{n}Y(E_{\gamma i})\int_{E_{min}}^{E_t(E_{\gamma i})}dE\int_{E_{min}}^{E_t(E_{\gamma i})}dE'\sigma(E_{\gamma i},E_{\gamma i}-E') \qquad (14)$$

where

N_0 is Avagadro's number,

d is the diameter of the emitter,

A is the atomic weight,

Z is the atomic number,

K is an approximation constant for the weighted average of the stopping energy over an appropriate energy range (200 keV to 6 MeV). For gadolinium, $K = 0.658\frac{gcm^2}{MeV}$,

$\bar{l}$ is the average path length, given as half the diameter for a gadolinium SPND, and

$\sigma(E_{\gamma i}, E_{\gamma i}-E')$ is the Compton scattering cross section and given in Equation 15.

23

$$\sigma(E_{\gamma i}, E_{\gamma i} - E') = \pi r_0^2 \frac{mc^2}{E_\gamma^2} \left[\frac{E_\gamma}{E_\gamma - E'} + \frac{E_\gamma - E'}{E_\gamma} + \left(\frac{mc^2}{E_\gamma - E'} - \frac{mc^2}{E_\gamma} \right)^2 \right.$$
$$\left. - 2 \left(\frac{mc^2}{E_\gamma - E'} - \frac{mc^2}{E_\gamma} \right) \right] \tag{15}$$

with $r_0^2 = 7.94e - 26 \ cm^2$.

The equation for the photoelectric effect contribution to the current is given in Equation 16.

$$I_{n,\gamma,e_{pe}} = \frac{\pi}{4} e d N_0 \frac{K}{\rho} \bar{l} R_n \sum_{i=1}^{n} Y(E_{\gamma i}) \mu(E_{\gamma i}) \left(E_{\gamma i} - E_k - E_{min} \right) \tag{16}$$

where ρ is the density of gadolinium, and $\mu(E_{\gamma i})$ is the approximation of the photoelectric effect cross section and given as

$$\mu(E_\gamma) = \frac{40\sqrt{2}}{3} \pi r_0^2 N Z^5 \left(\frac{1}{137} \right)^4 \left(\frac{mc^2}{E_\gamma} \right)^{7/2} \tag{17}$$

where N is the atomic density of the emitter.

2.3 Monte Carlo

The other methodology used to determine the electron current created from the SPND in this research is through Monte Carlo simulation, namely the Monte Carlo N Particle Transport (MCNP®) software. Monte Carlo simulations are conducted by proceeding through any number of probability functions. After proceeding through the probability functions, the result is tallied and the computer goes through the probability functions again. It repeats this process as many times as desired, ultimately determining the mean result and the associated variance.

2.4 TREAT

The TREAT facility at Idaho National Laboratory (INL) operated from 1959-1994 and was later refurbished and resumed operations in 2017 to support fuel safety testing as well as studying material structural responses to various levels and pulses of neutron flux. The TREAT facility is a air cooled, ziracloy-clad, graphite moderated reactor capable of almost any power history within 2500 MJ of max core transient energy [5], allowing it to stress the materials under test.

Typically, the residence time for a sample in the TREAT core for a given experiment is a few days; however, the transient neutron flux may last only a few milliseconds to minutes [5]. This short time period is why prompt SPNDs are used at this reactor instead of their more efficient counterpart.

To model the TREAT facility within MCNP®, the test cases and configuration used were the ones that matched the configuration during the Materials and Instruments Modular Irradiation Capability for Neutron detection (MIMIC-N) series of experimental tests, which were conducted to determine the operability and durability of neutron sensors, including the gadolinium SPNDs, during steady state and transient neutron fluxes [16]. The results and inputs of these tests are what were used to populate the TREAT, SPND model, and analytic models. The information gathered from these tests are also what is used to validate the output of all of the models used during research.

The reference neutron spectrum used for the analytic models is from these tests, and is shown in Figure 9 as well as Appendix B.
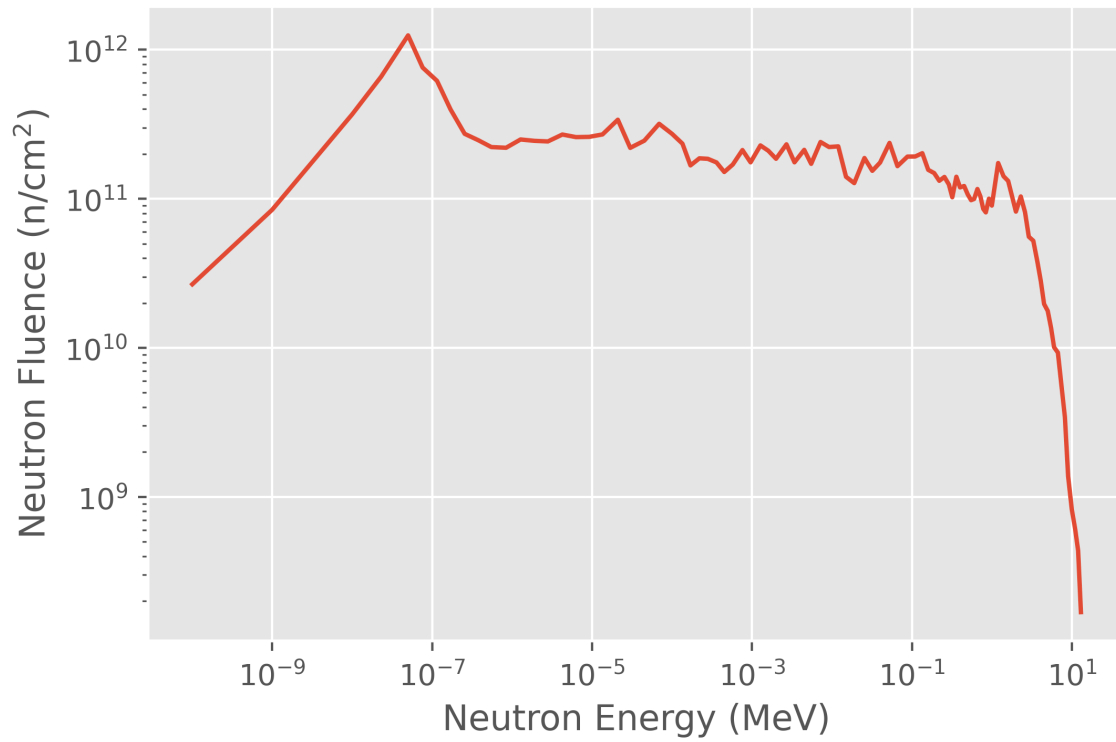
Figure 9. 100 group neutron spectrum of TREAT MIMIC-N 2959 [4]

III. Methodology

The methodology chapter covers how the Self Powered Neutron Detectors (SP-NDs) models were developed and incorporated into the full Transient REActor Test (TREAT) model, including how the sensitivity analysis was performed. This section also discusses what the results from the models will be compared to.

3.1   Modeling of the SPNDs

It is possible to turn on the electron mode within the TREAT model within Monte Carlo N Particle Transport (MCNP®) and collect the results of the electron current to the SPNDs. MCNP® can directly estimate the results; however, the computational time required would be excessive due to the large size of the model. To reduce the calculations needed and overall reduce computational time required, the dose response function was used within MCNP® to approximate how many electrons a source particle of a given energy would generate. To determine the dose response function, six models of the SPND were created: two models for each of the three main components of an SPND, the emitter, insulator, and collector. Two models were needed for each component to be able to separate the contributions from the neutron flux and the external gamma flux.

The data used to create the dose response function was determined through implementing a uniformly distributed 89 group or 48 group particle source for neutrons and photons respectively. These energy groups are tabulated in Appendix C and were chosen because they are commonly used for environments of interest. To create the data for the dose response function, the uniform distribution was used in conjunction with the SCX card within MCNP®, which tallies contribution according to the source particle energy group that caused the interaction [17].

The MCNP® version used for modeling the SPNDs was 6.2 and the nuclear data used were from the Evaluated Nuclear Data File (ENDF) VII.1 database [18].

3.1.1   DE/DF Card

To implement the dose response function within the TREAT MCNP® deck, the DE/DF card was used. This card takes source particle energy points and the respective data points, then interpolates to determine the response. While the interpolation can be linearly computed, due to the wide range on energies used, logarithmic interpolation was used instead. For the source particle energy point, the logarithmic bin center of the distribution was used. To handle data points that were zero, it was assumed that a small value, 1E-30, is functionally zero.

3.1.2   Insulator, Emitter, Sheath Modeling

All of the models had the source emitted inwardly from a sphere with a radius of 200 centimeters. While the sphere radius is somewhat arbitrary, it does need to be large enough to approximately isotropically irradiate the entirety of the geometry. The tally results must also be multiplied by πr^2, where r is the radius of the emitting sphere, to account for spherical divergence.

The emitter takes an F1 tally, which is the surface current tally with MCNP®, around the surface of the emitter to determine the number of electrons that are leaving the surface. It is assumed that the electric field of the insulator is created instantaneously, so the emitter model also removes electrons below 260 keV to account for that. This model assumes that the electrons that make it to the surface of the emitter (with energy greater than 260 keV) will make it to the sheath. The geometry used for the emitter model is illustrated in Figure 10 (not to scale).

28
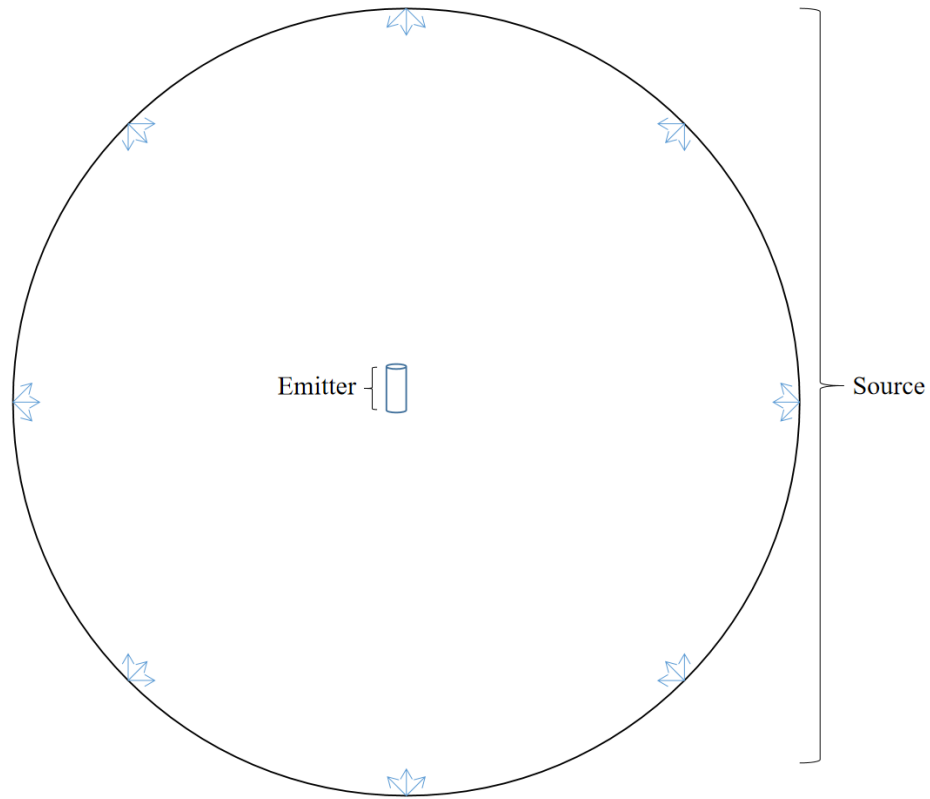
Figure 10. Illustration of MCNP® model for evaluating the dose response of the SPND's emitter (not to scale).

The insulator also takes an F1 tally around the surface between the insulator and the sheath. The insulator model includes the emitter, with the emitter's electron importance turned off to ensure that the contributions tallied are solely from the insulator. The geometry used for the insulator model is shown in Figure 11.

The sheath uses an F4 tally, which is the average cell flux tally within MCNP®, to calculate all electrons that are created within its volume, it also includes the insulator and the emitter with their electron importance set to zero so that the contributions tallied are solely from the sheath. The geometry used for the sheath model is shown in Figure 12.
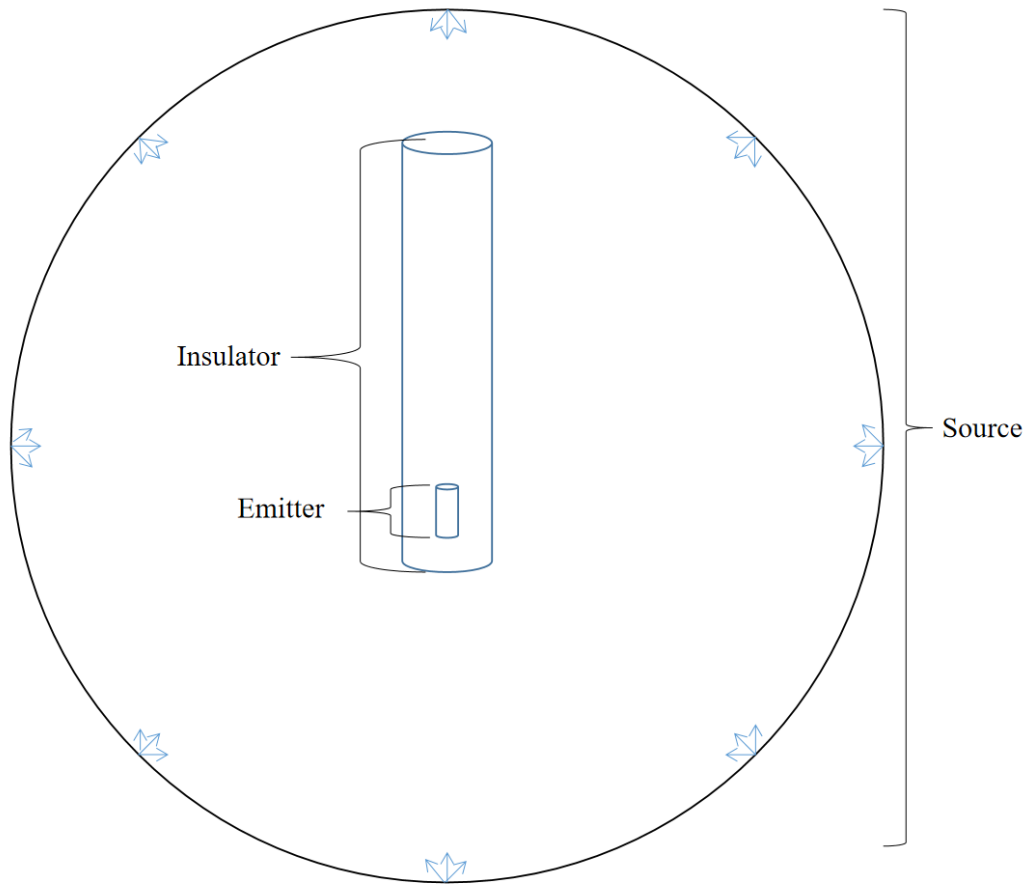
Figure 11. **Illustration of MCNP®️ model for evaluating the dose response of the SPND's insulator (not to scale).**

Once these tallies are obtained, they are multiplied by πr^2, the number of groups, and volume in the case of the sheath tally to remove spacial and tally that MCNP®️ inserts to obtain the total number of electrons tallied per source particle.

3.2 Uncertainty Propagation

To predict the energy current and determine how useful the methodology is, just using the mean of the SPND model results would be insufficient. Therefore, multiple dose response functions were created from each SPND result, the relative error was used to determine the 2σ variance, and those were also ran within TREAT.
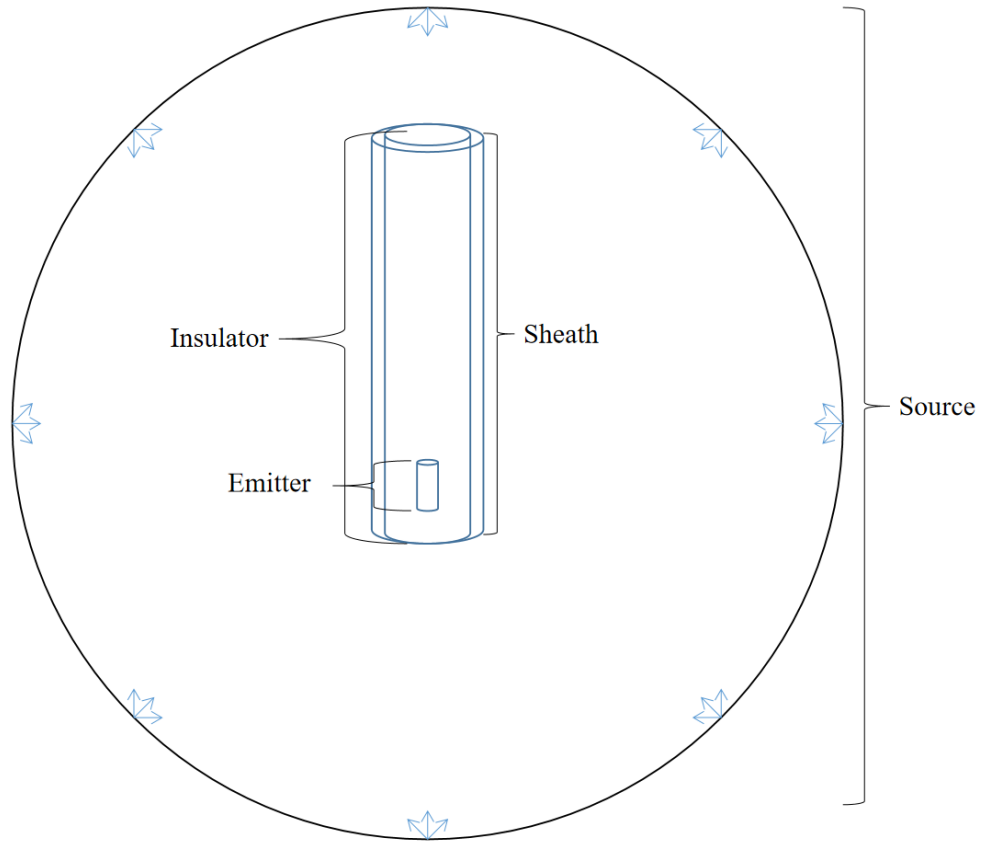
Figure 12. Illustration of MCNP® model for evaluating the dose response of the SPND's sheath (not to scale).

3.3 Validation Methodology

To validate the models, data obtained from the Materials and Instruments Modular Irradiation Capability for Neutron detection (MIMIC-N) test series is used and compared against the TREAT model results. The MIMIC-N test series were done to test the SPND and other measurement devices used in the TREAT facility. These series have gathered the experimental results showing that the SPNDs are linearly proportional to the total power of the reactor [19]. The results from the experiments found the relationship in Equation 18 and Equation 19 for type ILC4 and ILC6 of the gadolinium SPNDs respectively [16]:

$$I(nA) = 1.2309P(MW) - .0354 \tag{18}$$

and

$$I(nA) = 0.9256P(MW) - .0022 \tag{19}$$

where the power used during the reactor test, in MW, will determine the output current from the SPND, in nA.

To compare the model results to the experimental results, the DE/DF card in the TREAT model predicts the electron current per source particle. These results are then multiplied by the electron charge and the TREAT normalization parameters to determine the current per power. For this model of the reactor, it is assumed that there are about 7.6E16 neutrons per MW [14].

IV. Results and Analysis

The results chapter covers the data that was obtained from the modeling as well as how well the analytic models compare to them. This chapter also interprets what the data means and what information can be inferred to draw conclusions.

4.1 Monte Carlo N Particle Transport (MCNP®) Results

After running the model to determine the DE/DF card, Figure 13 and 14 show how the components react from a given neutron or photon energy respectively. These figures are made using the type ILC4 Self Powered Neutron Detector (SPND) geometry. The dash marks above and below the lines in the following figures indicate the upper and lower uncertainty bounds at 1σ.

All three of the components, the emitter, insulator, and sheath, react with largely just the thermal energy neutrons from Figure 13, which is expected due to neutron cross sections generally being larger at lower neutron energy. Furthermore, the emitter having more interactions is expected, as was seen in Figure 6, the (n,γ) cross section for the insulator and sheath were magnitudes lower than that of natural gadolinium. There were still many reactions; however, this is because the model for the sheath and the insulator included the emitter, the emitter absorbed the incoming neutrons and released the gamma rays that the insulator and sheath interacted with.

In Figure 14 it is seen that the photons start to react more commonly above a certain energy (around 100 keV), which is due to the inserted CUT card of 260 keV. While the total cross section increases with lower photon energies, the reaction becomes dominated by the photoelectric effect, which will completely absorb the photon to release an electron. So for low energy photons, the number of electrons produced is limited, while for a higher energy photon, the photon can create multiple

33

electrons to contribute to the current.

The current created by the photon interactions was also larger than the current created by the neutrons. This is expected since neutrons create photons after being absorbed by the gadolinium nucleus. The photons then release electrons through the photoelectric effect or Compton scatters. Therefore, the photon source distribution only requires one interaction, while the neutron source distribution requires another interaction to occur. This also means that when the results from the photon source are used in the dose response function, it will incorporate the external photon flux and also account for the neutron flux.

Figure 13. Neutron contributions of the ILC-4 SPND components.
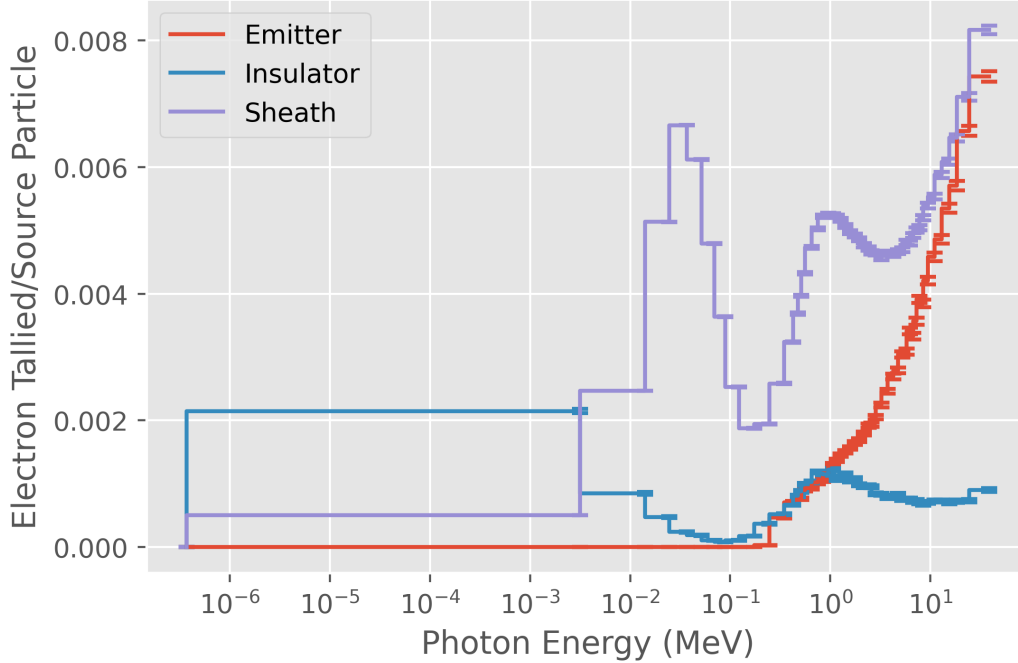
Figure 14. Photon contributions of the ILC-4 SPND components.

The neutron and photon MCNP® results for the type ILC6 SPND can be seen in Figure 15 and Figure 16 respectively. These results do not differ significantly from the type ILC4 SPND. The major difference is that the ILC4 has a larger emitter response compared to the ILC6 type detector, which is expected as the ILC4 has a length of 4.61 cm and the ILC6 has a length of 2.22 cm.

The relative errors of the neutron and photon contributions ($\sigma/\bar{x}$), where $\bar{x}$ is the mean, are plotted in Figure 17 and Figure 18 for the neutron and photon error respectively. These plots are using the error from the ILC4 SPND model as the relative error from the ILC6 model did not significantly differ from the ILC4 results. For the very large errors, those greater than 50%, only occur for neutron energies greater than 1 eV. As seen in Figure 13, incoming neutrons greater than 10^-4 MeV will have little impact on the results. While these errors are higher than the ideal maximum error of 10-20 %, nearing a 100% error at some energies, they were considered adequate due to time constraints and minimal impact to the total results.
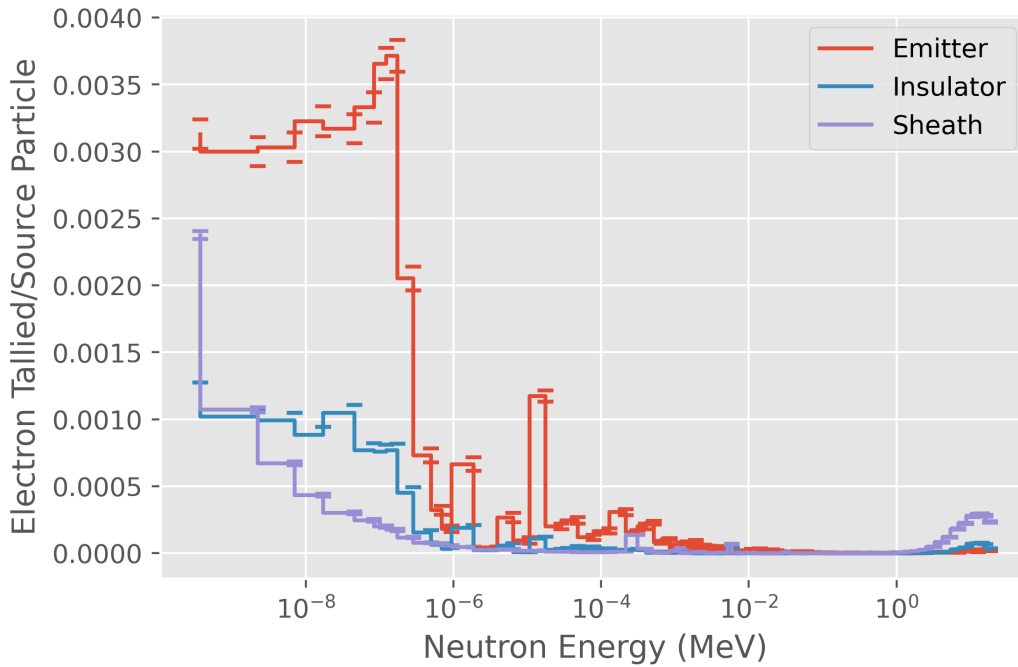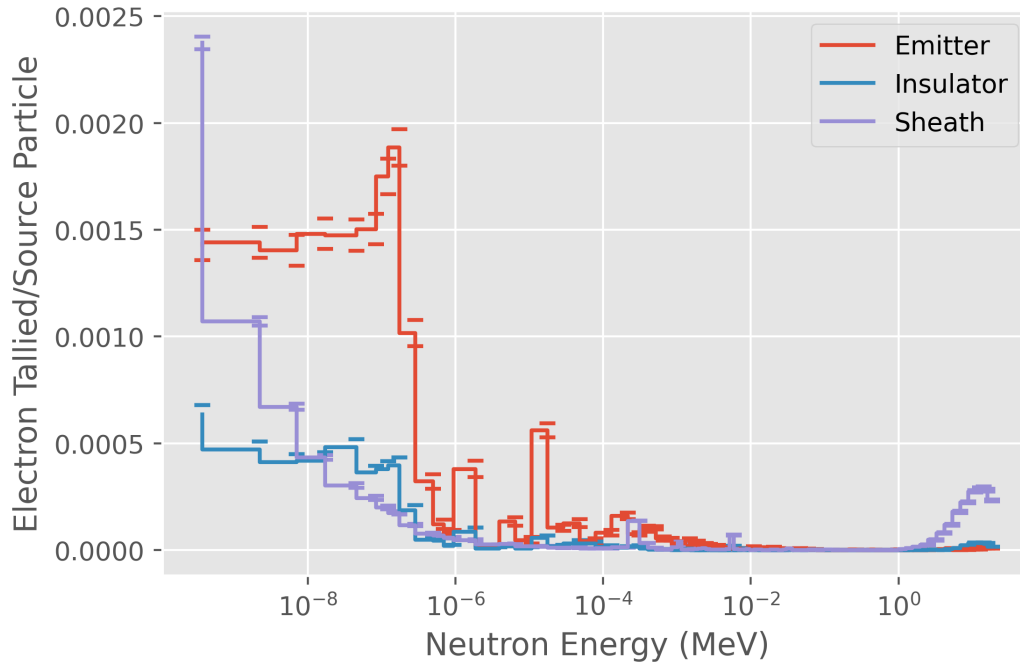
Figure 15. Neutron contributions of the ILC6 SPND components.
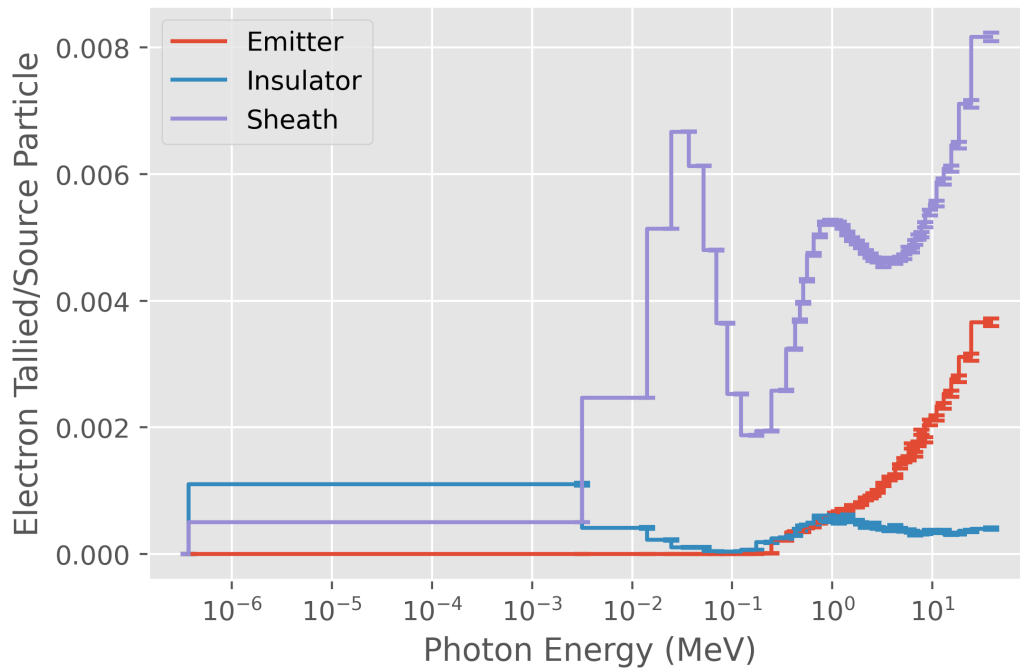
Figure 16. Photon contributions of the ILC6 SPND components.

36
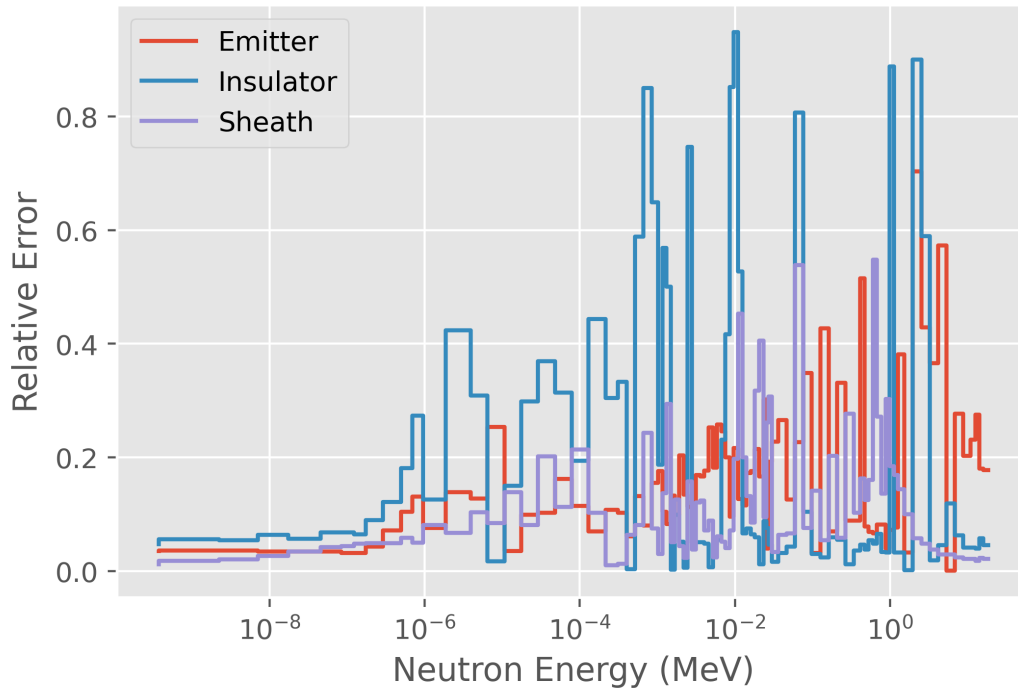
Figure 17. Relative error of the neutron contributions of the ILC4 SPND components.
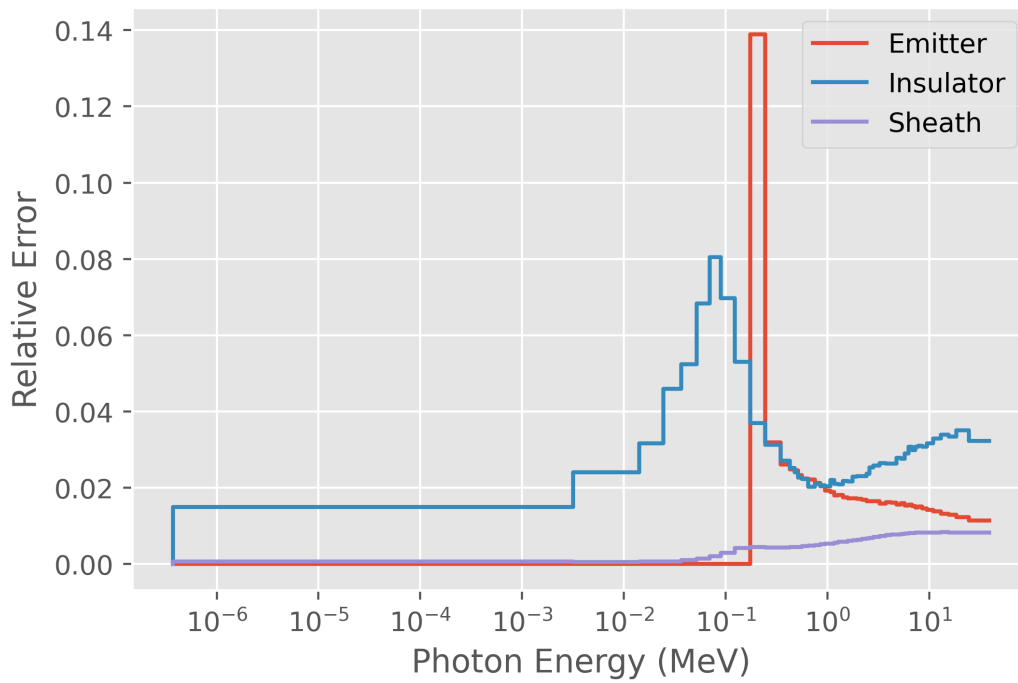
Figure 18. Relative error of the photon contributions of the ILC4 SPND components.

In the photon results, there is a notable spike in the error for the emitter at around 100 keV. This spike in error is due to the 260 keV CUT card that was used to simulate the electric field of the insulator. The error is not expected to create a high variance to the results due to the low contribution at this energy range.

4.1.1 Emitter

The emitter neutron contribution shown in Figure 13 and Figure 15 is larger than the neutron contribution from the insulator and the sheath. This is because the neutrons interact and release gamma rays in the emitter, as such the emitter is likely to interact with the gamma first, and also the highest energy gamma rays. For the emitter photon contribution shown in Figure 14 and 16, the emitter contribution is smaller than the sheath's contribution. While the emitter does have a large gamma cross section by about a magnitude than the sheath, as was shown in the gamma cross section figures, Figure 5 and Figure 8, the sheath has a much larger volume and not needing the electrons to travel results in a larger electron contribution.

It was expected that the emitter current to be proportional to length [8, 9] as the increase in length provides a larger surface area for neutrons and photons to interact with. Normalizing for the length of the emitter is shown below in Figures 19 and 20 for the neutron and photon tally respectively. It is seen that the contributions from the emitter are proportional to length.
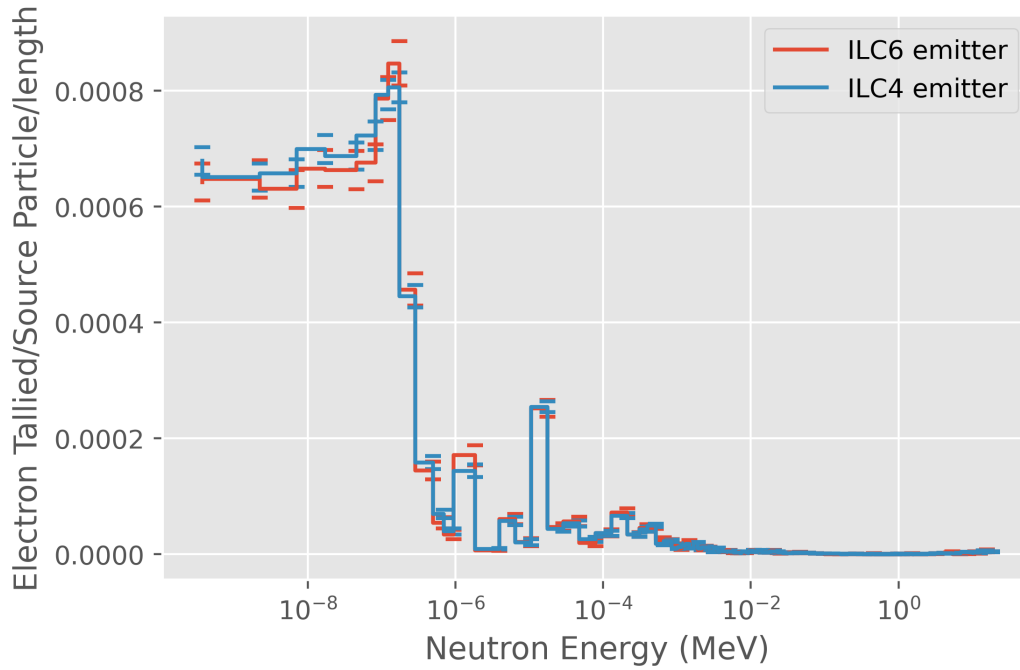
Figure 19. Length normalized emitter contribution due to neutron fluence.
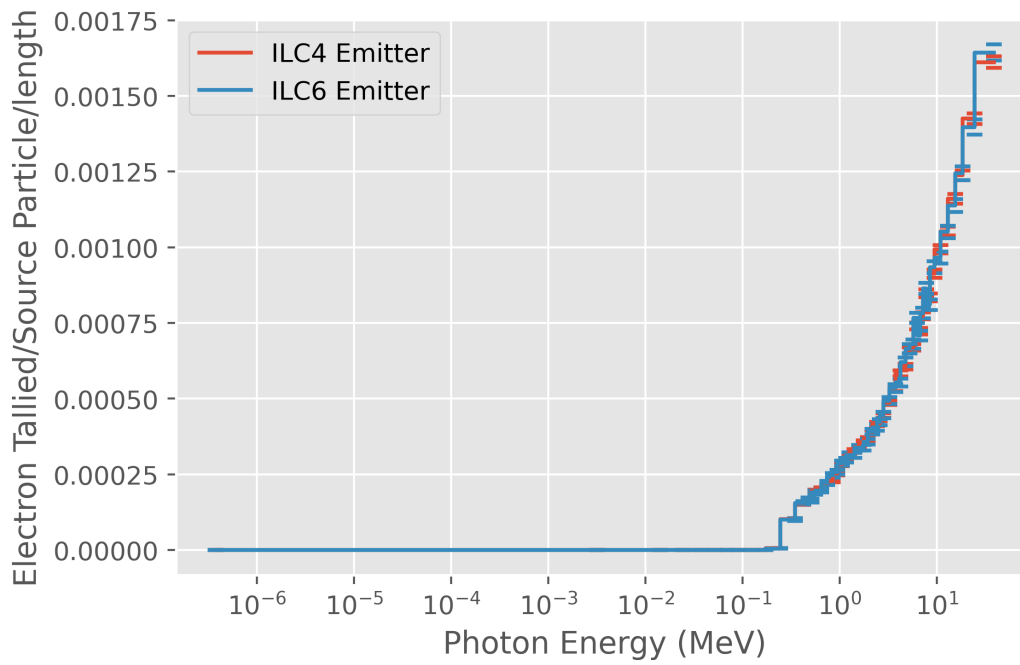
Figure 20. Length normalized emitter contribution due to photon fluence.

4.1.2 Insulator

When the neutrons were interacting with the insulator model, the contribution was found to be less by about half of the emitter model results. This contribution is due to the gamma ray macroscopic cross section of Al_2O_3 that was shown in Figure 7. The gamma rays that are not absorbed within the emitter travel through the insulator and have a decent of interacting and creating electrons. The insulator is mostly invisible to the neutron flux, and therefore is not creating a significant amount of gamma rays, but it is interacting with the gamma rays that are created in the emitter.

For the current from the external photon source distribution, the insulator is much smaller in contribution than the emitter and the sheath contributions. The insulator also has its highest contribution at the lowest photon energy, but this is due to how the model is constructed. The photons are streamed at insulator-sheath interface, so the low energy gamma rays will interact at that surface, and is more likely to be considered a contribution. However, the same low energy photon interacting at or near the insulator-emitter interface, would not be able to contribute to the current due to the insulator's electric field. In order to capture the external photon flux, this methodology was used instead of modeling photon emission from the emitter.

4.1.2.1 Insulator with the CUT card

As the insulator creates the electric field and depending on where the electron is created, the electron would feel the repulsive electric field away from the sheath. A CUT line was inserted within the MCNP® model at a radius determined from Equation 20 to simulate the electric field and prevent the model from counting low energy electrons that are created near the emitter [8]:

$$r = r_i \left[\frac{1 - (r_e/r_i)^2}{2ln(r_i/r_e)} \right]^2 \tag{20}$$

where r_i is the outer radius of the insulator, and r_e is the radius of the emitter.

Through comparison between running an insulator with a CUT card and one without, it can be shown that the difference, while measurable, is not significant due to the insulators small contribution. From Figure 21 and Figure 22, it is seen that the contribution from the neutron distribution has more variation than the photon distribution. This is also due to how the model is constructed, with the photon distribution being streamed at the surface of the insulator, while the majority of the photons that are created in the neutron distribution model are created by the emitter, and therefore are more likely to interact at the emitter-insulator surface and need the electron energy to pass through the electric field.
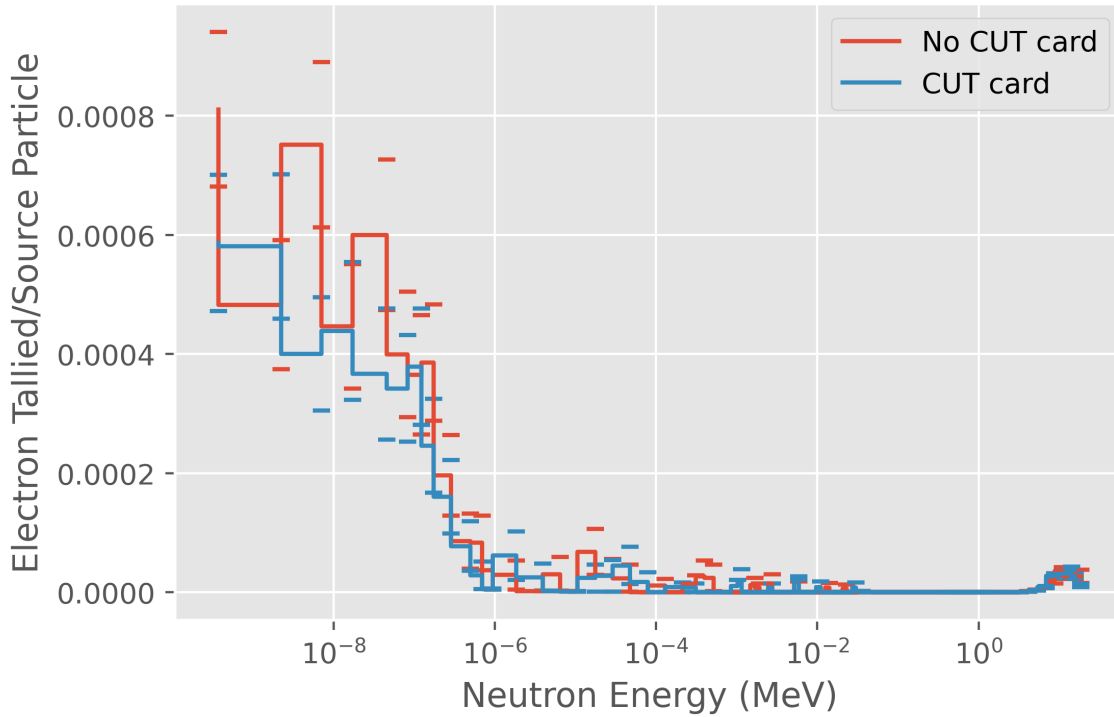
Figure 21. Neutron contribution comparison between insulator with a CUT line and without.
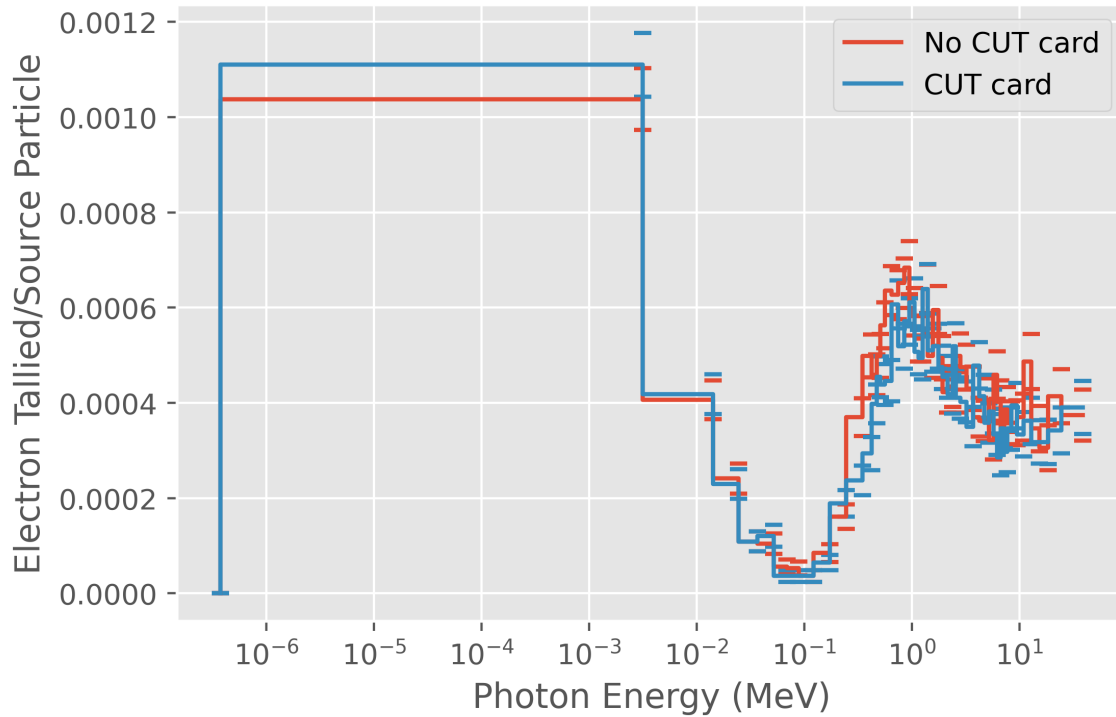
Figure 22. Photon contribution comparison between insulator with a CUT line and without.

4.1.3 Sheath

As discussed previously, the sheath contribution due to photons was found to be higher than the emitter contribution as seen in Figure 14 and 16, and that the size of the sheath makes it more likely for interactions to occur. It is also important to note that the sheath used an F4 tally, average volume flux, to determine the electron current. This tally was used as any electron that is within the sheath is counted as a charge, not just those that would cross the surface. However, the use of this tally means that any electrons that had too much energy imparted and ended up escaping the collector are not counted against the modeled contribution. Therefore, the sheath contribution is the most likely to be over-counting; however, even with the over count, it is not expected that the sheath would have a lower contribution than the other SPND components due to its larger size.

4.2 Comparison to MIMIC-N Experiments

After running the DE/DF tally card in the Transient REActor Test (TREAT) model, the results are tabulated in Table 5 and Table 6 for the ILC4 and ILC6 type SPND respectively. The error determined was by using the 2σ difference from the MCNP® model used to create the DE/DF card as well as the 2σ difference from the TREAT model. Most of the error is from determining the tally card, as was shown in Figure 17 and Figure 18, as the TREAT model had a relative error $(\sigma/\bar{x})$ of about 3% per tally.

There are two unexpected results from this set of data. The first is that the photon results are an order of magnitude larger than the neutron results. This is likely due to how the neutron model is limited in determining the total neutron contribution and reflecting gamma rays. As the model has a void around the component of interest, once the gamma ray leaves the component, it will not reflect back into the component and create more electrons. Therefore, the neutron results underestimate the number of photon interactions and resulting electrons that occur. These results do not mean that the current from gadolinium SPND is mostly due to the external photon flux, it means that the neutron dose response function is under counting its contribution by some unknown amount.

The second unexpected result is that the emitter contribution is an order of magnitude smaller than the sheath. This result is in part due to how large the sheath is compared to the emitter. The sheath is over 100 times greater than the ILC4 type emitter and 275 times greater than the ILC6 type emitter, therefore, even with a smaller cross section the sheath has a lot more opportunities to interact with either the gamma ray or the neutron particle. Furthermore, because the sheath doubles as the collector, any electron created within the sheath is counted towards the contribution while electrons created within the emitter must reach the surface with enough

43

energy to cross the insulator's electric barrier.

However, there are also possible errors in how the model determines the sheath contribution. A known error is that the model does not account for an electron escaping the collector and not ultimately contributing to the current. This methodology does mean that the sheath overestimates its contribution as it does not account for any electron escaping the collector; however, that serves to explain why the model overestimates the amount of current obtained. Even if the methodology accounted for electrons escaping the sheath, the sheath would likely still exceed that of the other components due to the difference in size.

Dividing the total current by the emitter length results in a mean current of 0.421 nA/cm/MW and 0.619 nA/cm/MW for the type ILC4 and ILC6 SPND respectively. Therefore, the total current is not proportional to the emitter length as a large amount of the current contribution is from the sheath. This result also implies that as the emitter length increases, the result is less efficient on a volume basis; however, there may be a point where the efficiency increases again as the emitter creates more photons for the other components to interact with. The sheath values do not change significantly with emitter length, but that may be because the emitter is too small. Once the emitter becomes sufficiently large it may significantly increase the sheath contributions.

The difference between the TREAT model results and the experimental results are close enough that the model is considered to be a good approximation. While the results has an absolute error of about 0.709 and 0.456 nA/MW for the type 4 and type 6 SPND respectively, the MCNP® modeling was expected to be inaccurate due to approximations in how MCNP® calculates electron transport as well as handling a lot of scatters and interactions as the delta rays and electrons interact with the components.

Table 5. Results from the TREAT MCNP® model for the ILC4 SPND

Particle	Component	Lower Bound (2σ)	Mean	Upper Bound (2σ)
Neutron	Emitter	0.036	0.0436	0.0511
Photon	Emitter	0.644	0.661	0.678
Both	Emitter	0.68	0.704	0.729
Neutron	Insulator	0.0065	0.00774	0.00896
Photon	Insulator	0.0115	0.0112	0.011
Both	Insulator	0.018	0.019	0.0199
Neutron	Sheath	0.0362	0.0396	0.043
Photon	Sheath	1.17	1.18	1.19
Both	Sheath	1.21	1.22	1.23
Neutron	All Components	0.0787	0.091	0.103
Photon	All Components	1.83	1.85	1.88
Both	All Components	1.9	1.94	1.98

The percent that each component contributes to the total current is shown in Table 7 and Table 8 for the ILC4 and ILC6 SPND respectively. As can be seen from Table 7 and Table 8, the emitter contribution is small for how important it was expected to be. Once again, this result does not account for the emitter producing photons through neutron absorption. Furthermore, it can be seen that the insulator contributes to about 1% or less of the total SPND current. Also, it was found that the emitter almost doubled their contribution from changing an emitter length of 2.23 cm to 4.61 cm.

Table 6. Results from the TREAT MCNP® model for the ILC6 SPND

Particle	Component	Lower Bound (2σ)	Mean	Upper Bound (2σ)
Neutron	Emitter	0.00835	0.011	0.0135
Photon	Emitter	0.139	0.144	0.149
Both	Emitter	0.147	0.155	0.163
Neutron	Insulator	0.0	0.0	0.0
Photon	Insulator	0.0	0.0	0.0
Both	Insulator	0.0	0.0	0.0
Neutron	Sheath	0.0335	0.0364	0.0394
Photon	Sheath	1.17	1.19	1.2
Both	Sheath	1.21	1.22	1.24
Neutron	All Components	0.0418	0.0474	0.0529
Photon	All Components	1.31	1.33	1.35
Both	All Components	1.36	1.38	1.4

Table 7. Percent of contribution for each ILC4 component

Particle	Component	Percent of Total
Neutron	Emitter	2.24
Photon	Emitter	34
Neutron	Insulator	0.398
Photon	Insulator	0.578
Neutron	Sheath	2.04
Photon	Sheath	60.7
Neutron	All Components	4.68
Photon	All Components	95.3

46

Table 8. Percent of contribution for each ILC6 component

Particle	Component	Percent of Total (%)
Neutron	Emitter	0.798
Photon	Emitter	10.5
Neutron	Insulator	0.0
Photon	Insulator	0.0
Neutron	Sheath	2.65
Photon	Sheath	86.1
Neutron	All Components	3.44
Photon	All Components	96.6

4.3   Analytic Results

The analytic models were constructed using the ILC6 SPND model, so the emitter has a length of 2.23 cm. The Warren analytic model was found to be much more time efficient than the Jaschik model, as expected due to the minimal amount of integrals that the Warren model uses. However, the Jaschik analytic model resulted in a much closer result to the MCNP® result for the emitter contribution due to neutrons. Figure 23 and Figure 24 show the difference in results between the two models by showing how they calculate the contribution agnostic of the incoming neutron flux.
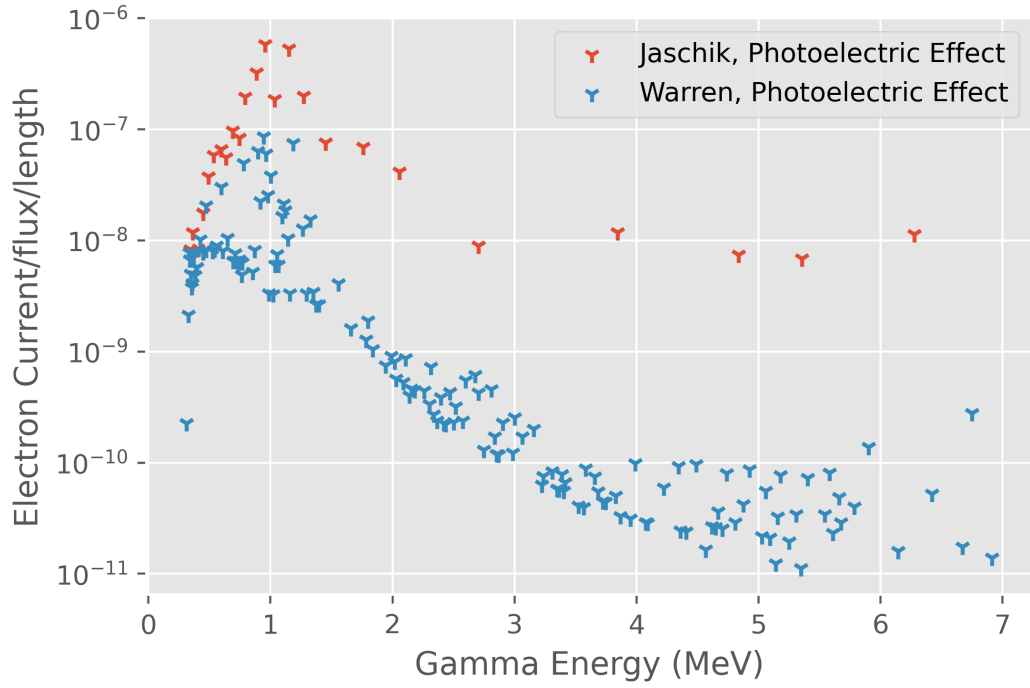
Figure 23. Photoelectric effect comparison between the Warren and Jaschik models
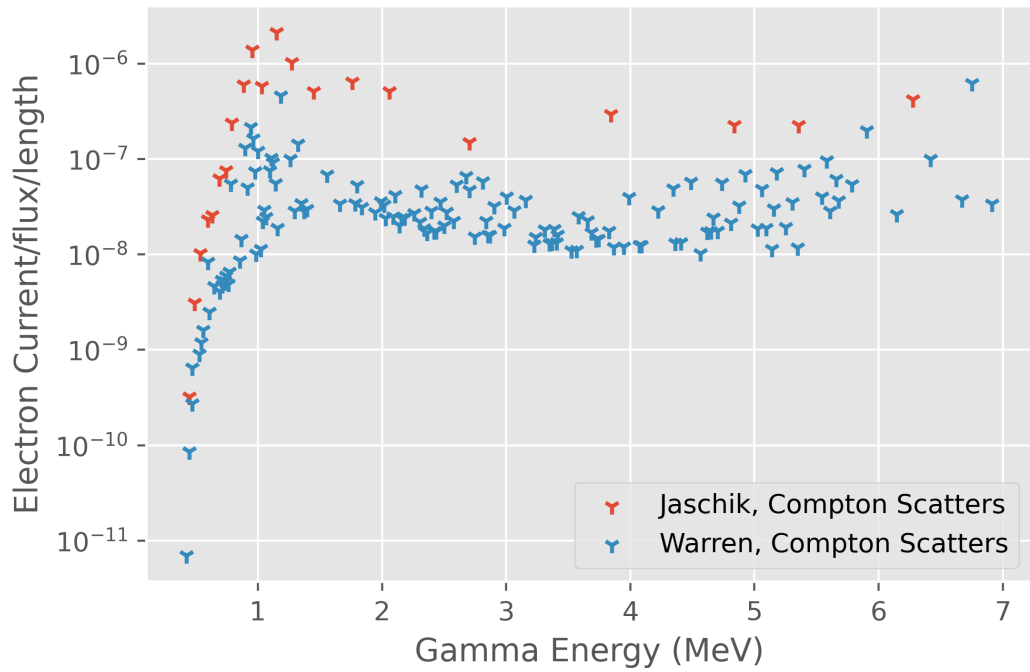
Figure 24. Compton scatter comparison between the Warren and Jaschik models

48

As seen in Figure 23 and Figure 24, the flux agnostic current varies significantly in small perturbations to the gamma ray energy. The variance is due to the yield factor not having any notable pattern as the gamma ray energy changes. The other two factors, the probability for a photon to collide (with either a Compton Scatter or Photoelectric Effect) and the probability for an electron to escape after creation, are smooth functions of the gamma ray energy. This is shown in Figure 25 and Figure 26 for the collision probability and escape probability respectively.
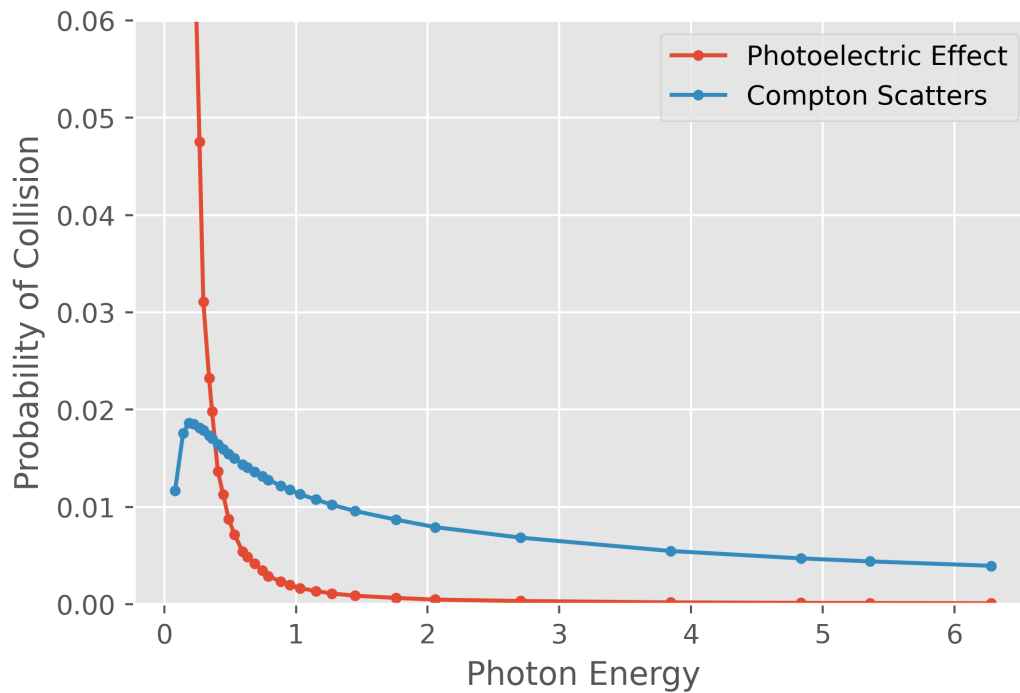
Figure 25. Probability of photon collision with the emitter as a function of photon energy
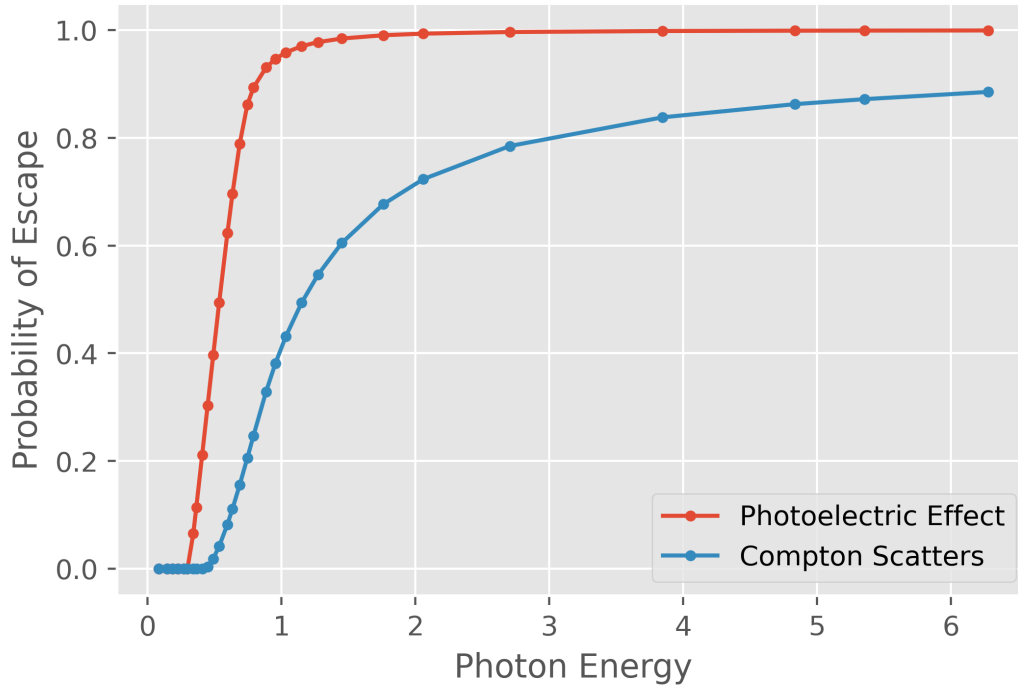
Figure 26. **Probability of electron escape from the emitter as a function of photon Energy**

The total result is found using the neutron fluence data of the Materials and Instruments Modular Irradiation Capability for Neutron detection (MIMIC-N) 2959 run [14], and the fluence is known to have resulted in a total power signature of about 254 MW. The results are tabulated below in Table 9. The Jaschik model results are extremely close to the SPND model for the emitter's current due to neutrons, 1.1E-2 nA/MW. The result is within 3σ of the mean. For the Warren model, it seems that the approximations made to reduce the calculation time make the model much more inaccurate than Jaschik's analytic method of grouping the prompt energy emissions into 30 groups. The usefulness of these models are unfortunately limited due to ignoring the contributions from the other effects and components.

The current can also be shown as a function of neutron energy, as seen in Figure 27. It can be seen that even though the Warren model is much larger than the Jaschik model, that the shapes of the two results are similar. It does deviate from the emitter

50

contribution shown in Figure 13 as there is not much of a contribution from neutrons with an energy greater than 10^{-7} MeV. The peak of the results is also matched by the fluence measured in the MIMIC-N experiment also peaking at close to the same energy.

Table 9. Jaschik and Warren analytical result for the ILC-6 SPND

Model	Current (nA/MW)	Absolute Error to the Mean (nA)
Warren	2.63E-2	1.5E-2
Jaschik	7.33E-3	3.3E-3
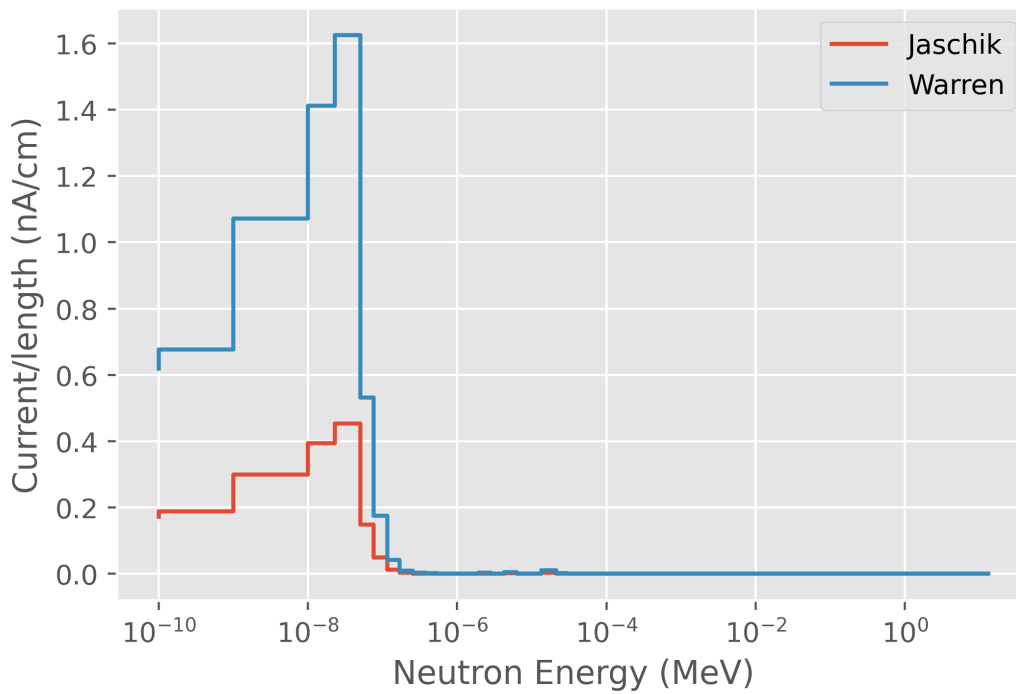
Figure 27. Total current comparison between the Warren and Jaschik models

V. Conclusions

The conclusion chapter summarizes the work done in this thesis as well as discussing some of the conclusions reached. This chapter also proposes future work that should be considered regarding Self Powered Neutron Detectors (SPNDs).

5.1   Summary

The primary objective of this research was to be able to identify, characterize, and quantify the influences of the individual components of a gadolinium SPND on the current and to compare these results to both real world experiments as well as the two analytic models created by Warren [9] and Jaschik [8]. Another objective was to be able to demonstrate that the gadolinium SPND current within Transient REActor Test (TREAT) can be adequately modeled using Monte Carlo N Particle Transport (MCNP®) with a dose response function to decrease the computation needs. Both of these objectives were met.

It was found that the sheath has the largest contribution to the current, contributing approximately 75% or 85% of the current for the ILC4 and ILC6 type SPND respectively. While this result was not expected, it should be noted that the emitter still plays a significant role in the SPND, as that is the material that will be interacting with the neutron flux and creating photons that the emitter or sheath may interact with to release electrons. The analytic model from Jaschik was also found to be fairly close to the MCNP® result for the emitter. However, because the emitter contribution due to neutrons was only 1.5% for either type of SPND, the usefulness of the analytical model may be limited.

Furthermore, the modeled results were within an order of magnitude of the experimental results, only being off by about +0.7 nA/MW and +0.5 nA/MW for the

ILC4 and ILC6 type respectively. This over estimation of the current is believed to be partially due to how the model was constructed and how MCNP® calculates electron transport. While these results could potentially be improved, they are still considered within expected error due to the limitations of MCNP® modeling and approximations made for electron transport and the computational effort of storing the results from a large amount of scatters.

5.2 Future Work

Future work regarding further validation studies is recommended. Also work in comparing models of different TREAT experiments or using different prompt SPND elements, such as hafnium, and replicating this methodology for delayed type SPNDs and comparing the results to literature on that topic as well as these results.

Other work could be in expanding the analytic models to account for the sheath. To expand the analytic model to account for the sheath, the path length probability for a hollow cylinder must be determined, the sheath should focus on the (γ, e⁻) reactions, and instead of multiplying by the probability of escape, the function would be multiplied by (1-P_{escape}).

The last project for researching SPNDs is in determining increases in efficiency for prompt SPNDs, work should be done in changing the geometry of the emitter to interact with more neutrons, as well as experiment with different materials of the sheath for increases in photon interaction.

For research regarding the methodology used in this research, further work is recommended using a different tool to model electron transport and use those results to create the dose response function.

Appendix A.   Gadolinium (n,γ) Yields

Table 10. Yield of a gamma ray at a specific energy from 100 neutron absorptions

γ Energy (MeV)	Yield
6.91	0.07
6.75	1.32
6.67	0.08
6.42	0.22
6.15	0.06
5.9	0.47
5.78	0.13
5.68	0.09
5.66	0.15
5.61	0.07
5.58	0.24
5.54	0.1
5.4	0.2
5.35	0.03
5.31	0.09
5.25	0.05
5.18	0.19
5.16	0.08
5.14	0.03
5.09	0.05
5.06	0.13
Continued on next page	

Table 10 – continued from previous page

γ **Energy (MeV)**	**Yield**
5.03	0.05
4.92	0.19
4.87	0.09
4.81	0.06
4.74	0.16
4.7	0.05
4.67	0.07
4.65	0.05
4.62	0.05
4.57	0.03
4.49	0.17
4.41	0.04
4.36	0.04
4.34	0.15
4.22	0.09
4.09	0.04
4.08	0.04
3.99	0.13
3.95	0.04
3.87	0.04
3.83	0.06
3.74	0.05
3.72	0.05
	Continued on next page

Table 10 – continued from previous page

γ **Energy (MeV)**	**Yield**
3.68	0.06
3.66	0.08
3.58	0.09
3.57	0.04
3.52	0.04
3.41	0.06
3.4	0.05
3.39	0.07
3.37	0.05
3.35	0.05
3.31	0.07
3.24	0.06
3.22	0.05
3.16	0.15
3.06	0.12
3.0	0.17
2.98	0.08
2.9	0.14
2.87	0.07
2.85	0.07
2.84	0.1
2.81	0.26
2.75	0.07

Table 10 – continued from previous page

γ Energy (MeV)	Yield
2.7	0.22
2.68	0.31
2.6	0.26
2.58	0.11
2.52	0.14
2.5	0.1
2.47	0.18
2.43	0.09
2.42	0.09
2.4	0.15
2.36	0.09
2.34	0.1
2.31	0.26
2.3	0.12
2.26	0.15
2.18	0.14
2.16	0.14
2.14	0.12
2.11	0.25
2.09	0.15
2.03	0.15
2.02	0.21
1.99	0.23

Table 10 – continued from previous page

γ Energy (MeV)	Yield
1.94	0.18
1.84	0.22
1.8	0.38
1.78	0.25
1.66	0.27
1.55	0.59
1.39	0.3
1.37	0.29
1.35	0.36
1.32	1.55
1.29	0.32
1.26	1.16
1.19	5.93
1.16	0.25
1.14	0.76
1.12	1.3
1.11	1.47
1.1	1.11
1.07	0.38
1.05	0.46
1.04	0.36
1.02	0.19
1.0	2.12

Table 10 – continued from previous page

γ Energy (MeV)	Yield
0.986	0.18
0.977	1.35
0.962	3.08
0.944	4.24
0.916	1.04
0.897	2.82
0.867	0.34
0.853	0.21
0.78	1.69
0.769	0.21
0.763	0.16
0.743	0.21
0.736	0.19
0.714	0.19
0.709	0.22
0.692	0.18
0.647	0.26
0.608	0.18
0.596	0.66
0.559	0.18
0.543	0.16
0.527	0.15
0.472	0.14
	Continued on next page

Table 10 – continued from previous page

γ Energy (MeV)	Yield
0.47	0.35
0.447	0.13
0.425	0.17
0.397	0.1
0.392	0.1
0.38	0.09
0.369	0.14
0.364	0.16
0.358	0.09
0.352	0.09
0.346	0.13
0.34	0.2
0.335	0.26
0.325	0.11
0.312	0.1
0.306	0.06
0.297	0.57
0.289	0.15
0.278	0.93
0.255	0.65
0.247	22.2
0.243	0.49
0.237	0.44

Table 10 – continued from previous page

γ **Energy (MeV)**	**Yield**
0.232	0.05
0.219	0.14
0.209	0.15

Appendix B. TREAT Neutron Fluence

Table 11. Neutron Flux per Unit Lethargy at the TREAT Facility

Neutron Energy (MeV)	Fluence per Unit Lethargy
1e-10	5.8e+08
1e-09	3.67e+10
1e-08	1.6e+11
2.3e-08	7.92e+11
5e-08	1.61e+12
7.6e-08	1.81e+12
1.15e-07	1.49e+12
1.7e-07	1.02e+12
2.55e-07	6.73e+11
3.8e-07	6.18e+11
5.5e-07	6.01e+11
8.4e-07	5.19e+11
1.28e-06	5.99e+11
1.9e-06	6.14e+11
2.8e-06	6.26e+11
4.25e-06	6.47e+11
6.3e-06	6.59e+11
9.2e-06	6.87e+11
1.35e-05	7.05e+11
2.1e-05	7.68e+11
3e-05	6.16e+11
Continued on next page	

Table 11 – continued from previous page

Neutron Energy (MeV)	Fluence per Unit Lethargy
4.5e-05	6.05e+11
6.9e-05	7.45e+11
0.0001	7.35e+11
0.000135	7.81e+11
0.00017	7.27e+11
0.00022	7.25e+11
0.00028	7.69e+11
0.00036	6.98e+11
0.00045	6.78e+11
0.000575	6.92e+11
0.00076	7.61e+11
0.00096	7.52e+11
0.00128	8.04e+11
0.0016	9.25e+11
0.002	8.32e+11
0.0027	7.73e+11
0.0034	7.62e+11
0.0045	7.6e+11
0.0055	8.55e+11
0.0072	8.93e+11
0.0092	9.08e+11
0.012	8.46e+11
0.015	6.3e+11

Table 11 – continued from previous page

Neutron Energy (MeV)	Fluence per Unit Lethargy
0.019	5.39e+11
0.0255	6.38e+11
0.032	6.78e+11
0.04	7.84e+11
0.0525	8.72e+11
0.066	7.24e+11
0.088	6.67e+11
0.11	8.61e+11
0.135	9.88e+11
0.16	9.21e+11
0.19	8.66e+11
0.22	9.01e+11
0.255	9.49e+11
0.29	9.7e+11
0.32	1.04e+12
0.36	1.19e+12
0.4	1.13e+12
0.45	1.03e+12
0.5	1.01e+12
0.55	1.03e+12
0.6	1.15e+12
0.66	1.22e+12
0.72	1.19e+12
	Continued on next page

Table 11 – continued from previous page

Neutron Energy (MeV)	Fluence per Unit Lethargy
0.78	1.07e+12
0.84	1.09e+12
0.92	1.1e+12
1.0	1.08e+12
1.2	9.53e+11
1.4	9.19e+11
1.6	9.86e+11
1.8	8.71e+11
2.0	7.79e+11
2.3	7.42e+11
2.6	6.63e+11
2.9	5.1e+11
3.3	4.05e+11
3.7	3.34e+11
4.1	2.72e+11
4.5	2.12e+11
5.0	1.68e+11
5.5	1.43e+11
6.0	1.16e+11
6.7	8.42e+10
7.4	5.71e+10
8.2	3.34e+10
9.0	1.48e+10
	Continued on next page

Table 11 – continued from previous page

Neutron Energy (MeV)	Fluence per Unit Lethargy
10.0	7.81e+09
11.0	6.41e+09
12.0	5.01e+09
13.0	2.11e+09

Appendix C. Neutron and Photon Energy Groups

Table 12. Neutron Energy Group Distribution

Group	Neutron Energy (MeV)
1	1.39e-10
2	1e-09
3	5e-09
4	1e-08
5	3e-08
6	7e-08
7	1e-07
8	1.52e-07
9	2e-07
10	4.14e-07
11	6e-07
12	8e-07
13	1.13e-06
14	3.06e-06
15	5.04e-06
16	8.32e-06
17	1.37e-05
18	2.26e-05
19	3.73e-05
20	6.14e-05
21	0.000101
	Continued on next page

Table 12 – continued from previous page

Group	Neutron Energy (MeV)
22	0.000167
23	0.000275
24	0.000354
25	0.000454
26	0.000583
27	0.000749
28	0.000961
29	0.00109
30	0.00123
31	0.0014
32	0.00158
33	0.0018
34	0.00203
35	0.00231
36	0.00261
37	0.00296
38	0.00335
39	0.0038
40	0.00431
41	0.00488
42	0.00553
43	0.00627
44	0.0071

Table 12 – continued from previous page

Group	Neutron Energy (MeV)
45	0.00805
46	0.00912
47	0.0103
48	0.0117
49	0.0133
50	0.015
51	0.017
52	0.0193
53	0.0219
54	0.0248
55	0.0261
56	0.0281
57	0.0318
58	0.0409
59	0.0525
60	0.0674
61	0.0865
62	0.111
63	0.143
64	0.183
65	0.235
66	0.302
67	0.388

Table 12 – continued from previous page

Group	Neutron Energy (MeV)
68	0.439
69	0.498
70	0.564
71	0.639
72	0.724
73	0.821
74	0.93
75	1.05
76	1.19
77	1.35
78	1.74
79	2.23
80	2.87
81	3.68
82	4.72
83	6.07
84	7.79
85	10.0
86	11.9
87	13.5
88	14.9
89	16.9
90	20.0

Table 13. Photon Energy Group Distribution

Group	Photon Energy (MeV)
1	0.001
2	0.01
3	0.02
4	0.03
5	0.045
6	0.06
7	0.08
8	0.1
9	0.15
10	0.2
11	0.3
12	0.4
13	0.45
14	0.5
15	0.525
16	0.6
17	0.7
18	0.8
19	0.9
20	1.0
21	1.12
	Continued on next page

Table 13 – continued from previous page

Group	Photon Energy (MeV)
22	1.2
23	1.33
24	1.5
25	1.66
26	1.88
27	2.0
28	2.33
29	2.5
30	2.67
31	3.0
32	3.5
33	4.0
34	4.5
35	5.0
36	5.5
37	6.0
38	6.5
39	7.0
40	7.5
41	8.0
42	9.0
43	10.0
44	12.0
	Continued on next page

Table 13 – continued from previous page

Group	Photon Energy (MeV)
45	14.0
46	17.0
47	20.0
48	30.0
49	50.0

Bibliography

1. C. Jensen, A. Crawford, K. Davis, A. Fleming, R. Fronk, L. Hone, N. Jerred, E. Larsen, R. Skifton, K. Tsai, T. Unruh, J. Roberts, M. Reichenberger, D. Nichols, W. Fu, and D. Mcgregor, "Fy18 report for instrumentation development for the transient testing program," 2018. [Online]. Available: http://www.inl.gov

2. "Photon cross section data for element/compound/mixture." [Online]. Available: https://physics.nist.gov/PhysRefData/Xcom/html/xcom1.html

3. "Gadolinium cross section data." [Online]. Available: https://atom.kaeri.re.kr/nuchart/?zlv=2#

4. T. Holschuh, S. Watson, and D. Chichester, "treat reactor metrology results from ctfw-4 and ctfw-5," Tech. Rep.

5. N. Woolstenhulme, "Capsule irradiations in treat," 2020.

6. W. H. Todt, "Characteristics of self-powered neutron detectors used in power reactors," in *Proc. of a Specialists' Meeting on In-core Inst. and Reactor Core Assessment, NEA Nuclear Science Committee*, 1996.

7. G. R. Imel and P. R. Hart, "The performance of hafnium and gadolinium self powered neutron detectors in the treat reactor*," pp. 325–336, 1996.

8. W. Jaschik and W. Seifritz, "model for calculating prompt-response self-powered neutron detectors," *Nuclear Science and Engineering*, pp. 61–78.

9. H. Warren and N. Shah, "Neutron and Gamma-Ray Effects on SPND in-core Reactors," *Nuclear Science and Engineering*, vol. 54, pp. 395–415, 1974.

10. H. D. Warren, "Calculational model for self-powered neutron detector," *NUCLEAR SCIENCE AND ENGINEERING*, vol. 48, pp. 331–342, 1970.

11. "Isotopes of gadolinium," 6 2021. [Online]. Available: https://en.wikipedia.org/wiki/Isotopes_of_gadolinium

12. "Thermal neutron capture gamma rays." [Online]. Available: https://www.nndc.bnl.gov/capgam/

13. T. Cui, Y. Yang, H. Xue, and H. Kuang, "A Monte-Carlo simulation method for the study of self-powered neutron detectors," *Nuclear Instruments and Methods in Physics Research*, vol. 954, 2020.

14. E. S. L. K Tsai, "Communications Regarding TREAT Capabilities and SPND Performances," 2021. Private Communications.

15. N. L. Snidow and H. D. Warren, "Wall Effect Corrections in Proportional Counter Spectrometers."

16. K. Tsai, L. Hone, and N. Woolstenhulme, "in-pile characterization testing of gadolinium self-powered neutron detectors," Tech. Rep.

17. C. Werner(editor), "MCNP Users Manual - Code Version 6.2," *Los Alamos National Laboratory*, 2017.

18. D. Brown, M. Chadwick, R. Capote, A. Kahler, A. Trkov, M. Herman, A. Sonzogni, Y. Danon, A. Carlson, M. Dunn, D. Smith, G. Hale, G. Arbanas, R. Arcilla, C. Bates, B. Beck, B. Becker, F. Brown, R. Casperson, J. Conlin, D. Cullen, M.-A. Descalle, R. Firestone, T. Gaines, K. Guber, A. Hawari, J. Holmes, T. Johnson, T. Kawano, B. Kiedrowski, A. Koning, S. Kopecky, L. Leal, J. Lestone, C. Lubitz, J. Márquez Damián, C. Mattoon, E. McCutchan,

S. Mughabghab, P. Navratil, D. Neudecker, G. Nobre, G. Noguere, M. Paris, M. Pigni, A. Plompen, B. Pritychenko, V. Pronyaev, D. Roubtsov, D. Rochman, P. Romano, P. Schillebeeckx, S. Simakov, M. Sin, I. Sirakov, B. Sleaford, V. Sobes, E. Soukhovitskii, I. Stetcu, P. Talou, I. Thompson, S. van der Marck, L. Welser-Sherrill, D. Wiarda, M. White, J. Wormald, R. Wright, M. Zerkle, G. Žerovnik, and Y. Zhu, "Endf/b-viii.0: The 8th major release of the nuclear reaction data library with cielo-project cross sections, new standards and thermal scattering data," *Nuclear Data Sheets*, vol. 148, pp. 1–142, 2018, special Issue on Nuclear Reaction Data. [Online]. Available: https://www.sciencedirect.com/science/article/pii/S0090375218300206

19. J. A. King, A. M. Miller, and E. J. Parma, "spnd sensitivity calculations using mcnp and experimental data from acrr sandia national laboratories," Tech. Rep.

REPORT DOCUMENTATION PAGE

1. REPORT DATE *(DD–MM–YYYY)*	2. REPORT TYPE	3. DATES COVERED *(From — To)*
24–03–2022	Master's Thesis	Sept 2020 — Mar 2022

4. TITLE AND SUBTITLE	5a. CONTRACT NUMBER
Modeling and Validation of Gadolinium Self Powered Neutron Detectors in a Transient Reactor	5b. GRANT NUMBER 89233119SNA000103 5c. PROGRAM ELEMENT NUMBER

6. AUTHOR(S)	5d. PROJECT NUMBER
Spring, Alexander L., Capt, USAF	5e. TASK NUMBER 5f. WORK UNIT NUMBER

7. PERFORMING ORGANIZATION NAME(S) AND ADDRESS(ES)	8. PERFORMING ORGANIZATION REPORT NUMBER
Air Force Institute of Technology Graduate School of Engineering an Management (AFIT/EN) 2950 Hobson Way WPAFB OH 45433-7765	AFIT-ENP-MS-22-M-111

9. SPONSORING / MONITORING AGENCY NAME(S) AND ADDRESS(ES)	10. SPONSOR/MONITOR'S ACRONYM(S)
National Nuclear Security Administration 1000 Independence Ave, S.W. Washington D.C. 20585	NNSA
	11. SPONSOR/MONITOR'S REPORT NUMBER(S)

12. DISTRIBUTION / AVAILABILITY STATEMENT

DISTRIBUTION STATEMENT A:
APPROVED FOR PUBLIC RELEASE; DISTRIBUTION UNLIMITED.

13. SUPPLEMENTARY NOTES

14. ABSTRACT

Contributions to the electron current from the three components of a gadolinium SPND, emitter, insulator, and sheath, are identified, characterized, and quantified to provide information on how the SPND interacts within the transient neutron and photon flux of the TREAT to create a measurable current. These contributions are measured by defining the SPND interactions as a dose response function used within a Monte Carlo simulation of a TREAT experiment. The data obtained from the Monte Carlo simulations are then used to compare against two analytic models, developed by Jaschik and Warren, as well as the experimental results. It was found that the methodology used produced sufficiently accurate results, that the sheath has the highest total contribution to the current, and that while the analytic models sufficiently predict the emitter contribution, they have a very limited use due to not accounting for the sheath.

15. SUBJECT TERMS

Monte Carlo simulations, Self Powered Neutron Detector, TREAT

16. SECURITY CLASSIFICATION OF:			17. LIMITATION OF ABSTRACT	18. NUMBER OF PAGES	19a. NAME OF RESPONSIBLE PERSON
a. REPORT	b. ABSTRACT	c. THIS PAGE			Dr. Whitman Dailey, AFIT/ENP
U	U	U	UU	88	19b. TELEPHONE NUMBER *(include area code)* (937) 255-3636 x4586; whitman.dailey@afit.edu